

Click Co Sandwich-Terminated Dendrimers as Polyhydride Reservoirs and Micellar Templates

Amalia Rapakousiou, Colette Belin, Lionel Salmon, Jaime Ruiz, Didier Astruc*

Electronic Supplementary Information (ESI)

Contents:

1.	General data	S04
2.	Preliminary studies using benzylmethyl-(trz-η^4-C₅H₅Co^ICp)	S05
	Synthesis of benzylmethyl-(trz-η^4-C₅H₅Co^ICp)	S05
	UV-vis. studies	S07
	Mass spectrometry studies	S08
	¹ H NMR of benzylmethyl-(trz-η^4-C₅H₅Co^ICp)	S09
	Oxidation of benzylmethyl-(trz-η^4-C₅H₅Co^ICp)	S10
	ESI MS spectra studies	S10
	Cyclic voltammetry studies	S11
	Synthesis of benzylmethyl(triazolyl)-η^5-C₅H₄Co^{III}Cp (Cl)	S12
	¹ H NMR of benzylmethyl(triazolyl)- η^5-C₅H₄Co^{III}Cp (Cl)	S13
	UV-vis. of benzylmethyl(triazolyl)- η^5-C₅H₄Co^{III}Cp (Cl)	S14
	¹ H NMR of molecular hydrogen during oxidation to benzylmethyl(triazolyl)-η^5-C₅H₄Co^{III}Cp (Cl)	S15
3.	Filled DHR 4	S16
	Experimental procedure for DHR 4	S17
	UV-vis. of DHR 4	S18
	IR of DHR 4	S19
	ESI MS of DHR 4	S20
	AFM studies of DHR 4	S21
	¹ H NMR spectrum of DHR 4	S23
	¹³ C NMR spectrum of DHR 4	S24
	HSQC 2D NMR of DHR 4	S25
4.	Filled DHR 5	S26
	Experimental procedure for DHR 5	S27
	UV-vis. of DHR 5	S28
	IR of DHR 5	S29
	AFM studies of DHR 5	S30
	¹ H NMR spectrum of DHR 5	S31
	¹³ C NMR spectrum of DHR 5	S32
	HSQC 2D NMR of DHR 5	S33
5.	Filled DHR 6	S34
	Experimental procedure for DHR 6	S34
	AFM studies of DHR 6	S34

UV-vis. of DHR 6	S35
IR of DHR 6	S36
6. Empty DHR 1(Cl)	S37
Experimental procedure for DHR 1(Cl)	S38
¹ H NMR spectrum of DHR 1(Cl)	S39
UV-vis. of DHR 1(Cl)	S40
IR of DHR 1(Cl)	S41
7. Empty DHR 2(Cl)	S42
Experimental procedure for DHR 2(Cl)	S43
UV-vis. of DHR 2(Cl)	S44
¹ H NMR spectrum of DHR 2(Cl)	S45
8. Empty DHR 3(Cl)	S46
Experimental procedure for DHR 3(Cl)	S46
¹ H NMR spectrum of DHR 3(Cl)	S47
UV-vis. of DHR 3(Cl)	S48
9. AuNPs-7 and AuNPs-8	S49
General information	S49
Experimental procedure of AuNPs-7 and AuNPs-8	S50
UV-vis. of AuNPs-7	S51
TEM of AuNPs-7	S52
Size distribution of AuNPs-7	S53
UV-vis. of AuNPs-8	S54
Size distribution of AuNPs-8	S55
AFM studies of AuNPs-8	S56
10. AuNPs-9	S58
General information	S58
Experimental procedure for AuNPs-9	S59
Size distribution of AuNPs-9	S60
11. AuNPs-10	S61
General information	S62
Experimental procedure of AuNPs-10	S63
TEM of AuNPs-10	S64
Size distribution of AuNPs-10	S64
UV-vis. of AuNPs-10	S65
12. Stability comparison of AuNPs-8 and AuNPs-10	S66
UV-vis of AuNPs-8 after 6 months	S66
UV-vis. of AuNPs-8 after heating at 100°C during 1h	S67
13. AuNPs-11 and AuNPs-12	S68
General information	S68
Experimental procedure for AuNPs-11	S69
UV-vis. of AuNPs-11	S70
TEM of AuNPs-11	S71

Size distribution of AuNPs-11	S72
Oxidation of AuNPs-11 to AuNPs-12 (experimental procedure)	S73
TEM of AuNPs-12	S74
Size distribution of AuNPs-12	S75
UV-vis. of AuNPs-12	S76

14. References	S77
-----------------------	-----

ABBREVIATIONS :

DHR : Dendritic hydride reservoir
DER : Dendritic electron reservoir
IR : Infrared spectroscopy
CV : Cyclic voltammogram
TEM : Transmission electron microscopy
AFM : Atomic force microscopy
Trz : 1,2,3-Triazolyl group
MS : Mass spectrum
DCM : Dichloromethane
UV-vis. : UV-visible
AuNPs : Gold nanoparticles
AgNPs : Silver nanoparticles
PdNPs : Palladium nanoparticles

General data

Reagent-grade tetrahydrofuran (THF) was predried over Na foil and distilled from sodium-benzophenone anion under argon immediately prior to use. All other solvents and chemicals were used as received.

The ^1H NMR spectra were recorded at 25°C with a Bruker AVANCE II 400 MHz spectrometer. The ^{13}C NMR spectra were obtained in the pulsed FT mode at 100 MHz with a Bruker AVANCE 400 spectrometer. All chemical shifts are reported in parts per million (δ , ppm) with reference to Me_4Si (TMS). The infrared (IR) spectra were recorded on an ATI Mattson Genesis series FT-IR spectrophotometer.

The mass spectra were performed at the CESAMO (University of Bordeaux, France) on a QStar Elite mass spectrometer (Applied Biosystems). The instrument is equipped with an ESI source, and spectra were recorded in the positive mode. The electrospray needle was maintained at 5000V and operated at room temperature. Samples were introduced by injection through a 20 μL sample loop into a 4500 $\mu\text{L}/\text{min}$ flow of methanol from the LC pump. The mass spectrum of benzylmethyl-($\text{trz-}\eta^4\text{-C}_5\text{H}_5\text{Co}^1\text{Cp}$) was recorded by the CESAMO on a AccuTOF- GcV (JEOL) that is a GC-TOF. The instrument is equipped with a sample introduction system named FD (Field Desorption). The MALDI-TOF mass spectra were performed on a PerSeptive Biosystems Voyager Elite (Framingham, MA) time of flight mass spectrometer.

All electrochemical measurements (CV) were recorded under the following conditions. Solvent: dry DMF; temperature: 20°C; supporting electrolyte: [$n\text{Bu}_4\text{N}$][PF_6] 0.1M; working and counter electrodes: Pt; reference electrode: Ag; internal reference: FeCp^*_2 ($\text{Cp}^* = \eta^5\text{-C}_5\text{Me}_5$); scan rate: 0.200 $\text{V}\cdot\text{s}^{-1}$.

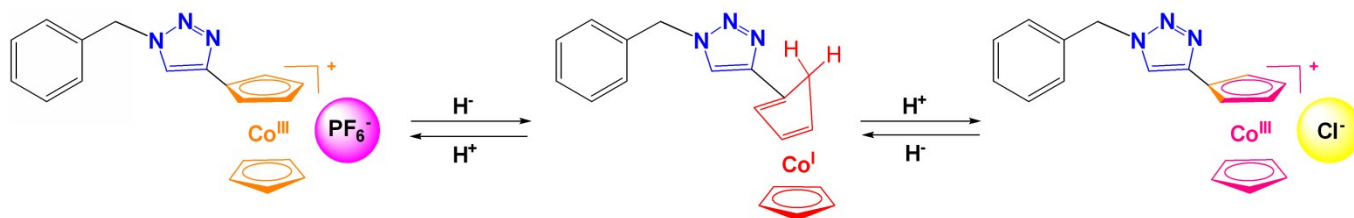
UV-visible: UV-visible absorption spectra were measured with a Perkin-Elmer Lambda 19 UV visible spectrometer.

AFM of filled DHR 4, 5 and 6: All measurements were made using tapping mode operation with an Agilent Technologies 5500 microscope and a Nanosensor ‘‘PPP-NCL®’’ TIP.

AFM of AuNPs-8: Dimension ICON (BRUKER), mode PEAK FORCE TAPPING (exclusivity BRUKER): every interaction between tip and sample is analyzed, allowing the benefits of Peak Force Tapping. Modulus, adhesion, dissipation, deformation are mapped simultaneously with topography. Individual curves can be examined and analyzed offline (5peakForce Capture). Nanosensor tip used: ‘PFQNE-AI’.

Preliminary studies:

A triazolyl-cobalticinium (Co^{III}) model (benzyl-methyl-triazolylcobalticinium hexafluorophosphate) proved to be an efficient hydride reservoir ($\pm\text{H}^-$). The stability of the reduction product (Co^{I}) and the reversibility of the system ($\text{Co}^{\text{I}}/\text{Co}^{\text{III}}$) is of utmost importance when similar procedures are envisaged for large nanosystems.



Scheme S1: Reaction of **benzyl-methyl-triazolyl($\eta^5\text{-C}_5\text{H}_4\text{Co}^{\text{III}}\text{Cp}$)** with NaBH_4 giving the neutral **benzylmethyl-(trz- $\eta^4\text{-C}_5\text{H}_5\text{Co}^{\text{I}}\text{Cp}$)** product by addition of an hydride on the Cp ring, which then in the presence of a protonic source will react with H^+ giving back the cationic product benzyl-methyl-triazolyl($\eta^5\text{-C}_5\text{H}_4\text{Co}^{\text{III}}\text{Cp}$) $^+$ (X^-) by production of molecular hydrogen. ($\text{Cp} = \eta^5\text{-C}_5\text{H}_5$)
 $\text{X}^- = \text{PF}_6^-$ or Cl^- . A single Co^{I} isomer is represented. For the structures of the four isomers, see Figure S1.

Synthesis of benzylmethyl-(trz- $\eta^4\text{-C}_5\text{H}_5\text{Co}^{\text{I}}\text{Cp}$)

The reduction of this ‘model’ monomer benzyl-triazolyl-cobalticinium hexafluorophosphate compound was studied in order to test if the triazole ligand is stable under these conditions. The orange cationic compound reacted in THF with NaBH_4 to produce the wine-red neutral triazolyl η^4 -cyclopentadiene-cobalt(I)- η^5 -cyclopentadienyl complex according to equation (S1).



The color of the orange solution changed to wine-red and the neutral product benzylmethyl-(trz- $\eta^4\text{-C}_5\text{H}_5\text{Co}^{\text{I}}\text{Cp}$) was extracted in distilled diethyl ether under N_2 in which NaPF_6 salt –also formed- was not soluble. The addition of the hydride anion is added onto four different carbons of the Cp ring, providing isomers (figure S1).

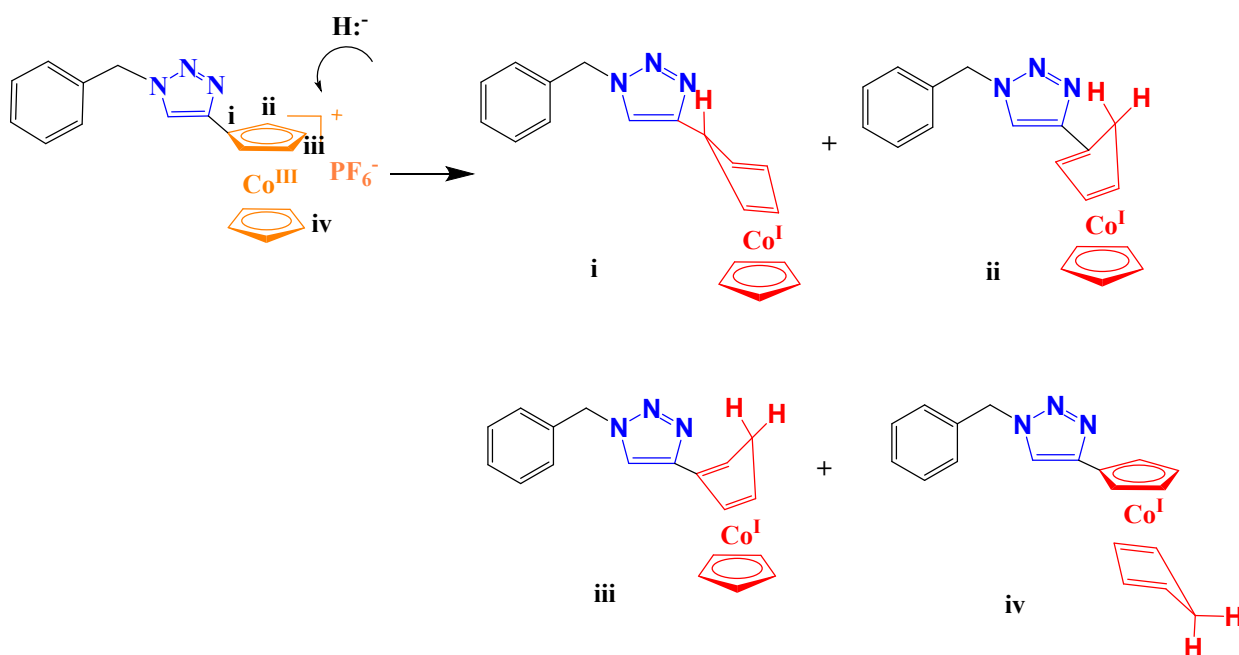


Figure S1: Addition of a hydride anion occurs onto four different positions: i) ipso, ii) 1,2 or iii) 1,3 position of the cyclopentadienyl ligand attached to the triazole or iv) onto the free cyclopentadienyl ligand.

Experimental procedure¹:

A mixture of 1 equiv. of benzylmethyl(triazolyl)- $\eta^5\text{-C}_5\text{H}_4\text{Co}^{\text{III}}\text{Cp}(\text{PF}_6)$ (150 mg, 0.31mmol) with 1.1 equiv. of NaBH_4 (12.71 mg, 0.34mmol) in distilled THF (20 mL) was stirred for 20 min at 0°C under N_2 . Then, the solvent was evaporated under vacuum, and distilled diethyl ether was added to solubilize the neutral product. After filtration under N_2 and evaporation of the solvent, the product was obtained as a deep red powder; yield 95%. ^1H NMR (1D, 1H) CDCl_3 , 400 MHz: $\delta = 7.41\text{--}7.31$ (5H, CH of Ph), 7.13 and 6.66 (1H of trz), 5.51–5.34 (2H of Ph- CH_2 and 2H of diene), 4.88–4.52 (5H of free Cp and 4H of substituted Cp when H^- is added to free Cp), 2.93–2.88 (2H of diene), 2.09–2.04 (2H free) ppm.

UV-Vis. studies

The UV-vis spectroscopic technique proved to be an excellent way to differentiate the cationic benzylmethyl(triazolyl)- η^5 -C₅H₄Co^{III}Cp(PF₆) compound from the benzylmethyl-(trz- η^4 -C₅H₅Co^ICp) neutral compound. The hydride addition on the Cp ring of the cobalticenium complex leading to the neutral CpCo^I η^4 -cyclopentadiene causes a push-pull electronic effect between the electron-withdrawing triazolyl group and the electron-donor CpCo^Icyclopentadiene group. This results in a bathochromic shift (red shift) of the two absorption bands of the cationic compound at 350 nm and 420 nm in the UV-vis. spectrum that moved to 410 nm and 520 nm respectively. The absorption band at 410 nm is assigned to the d-d* transitions of the cobalt complex, whereas the band appearing at 530 nm is assigned to the d-d* transitions mixed with charge transfer from the ligand to the metal (L→MCT).

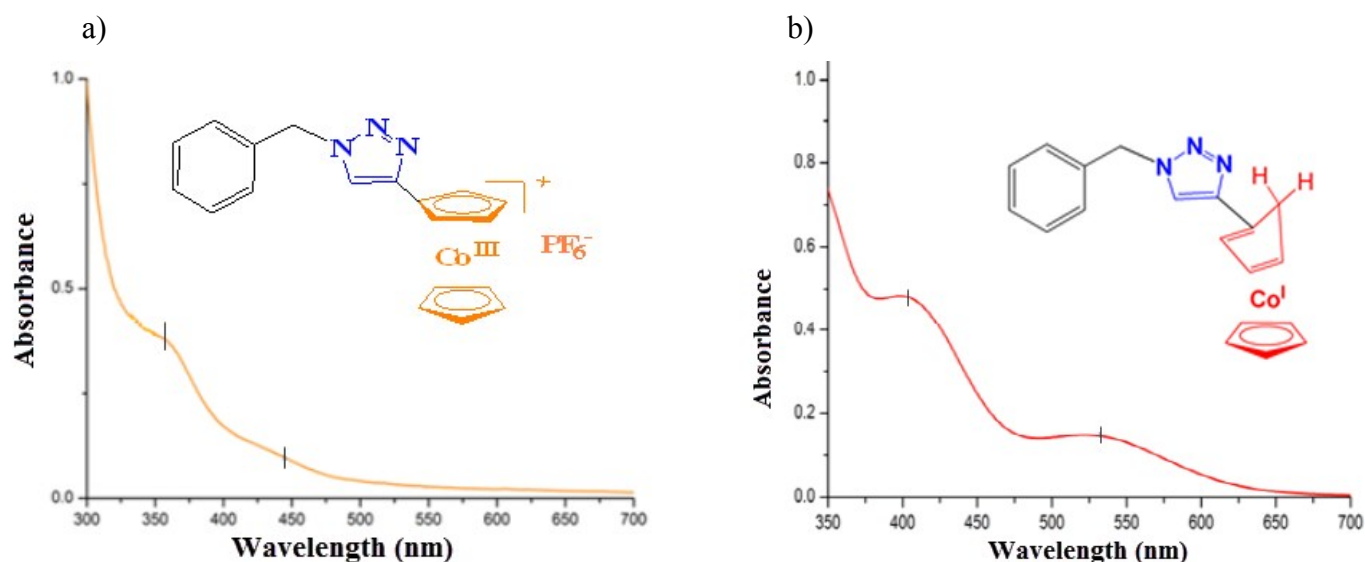


Figure S2: UV-vis. spectra of a) benzylmethyl(triazolyl)- η^5 -C₅H₄Co^{III}Cp(PF₆) and b) the benzylmethyl-(trz- η^4 -C₅H₅Co^ICp) compounds (a single isomer is represented, for the isomer structures, see Figure S1).

Mass spectrometry studies

The mass spectrum of benzylmethyl-(trz- η^4 -C₅H₅Co^ICp) was performed at the CESAMO on a AccuTOF- GeV (JEOL) that is a GC-TOF. The instrument is equipped with a sample introduction system named FD (Field Desorption).

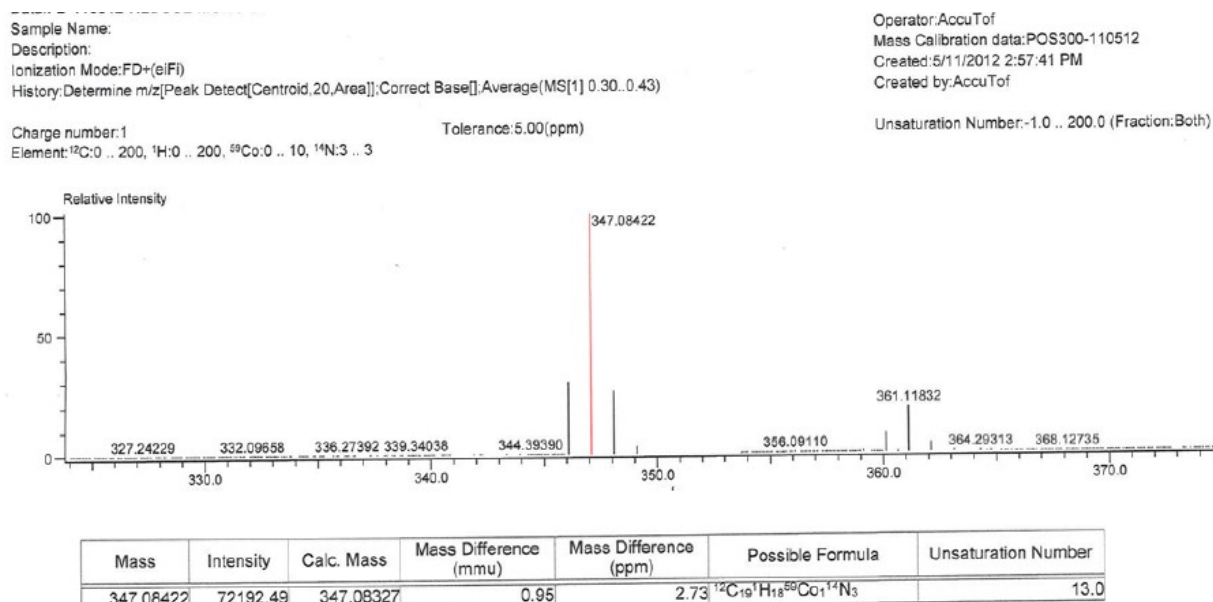


Figure S3: FD MS of neutral benzylmethyl-(trz- η^4 -C₅H₅Co^ICp) (M = 347 Da), showing the successful addition of the hydride onto the complex benzylmethyl(triazolyl)- η^5 -C₅H₄Co^{III}Cp (PF₆) for which the calculated mass is 346 Da^[1].

^1H NMR of benzylmethyl-(trz- η^4 -C₅H₅Co^ICp)

NMR spectroscopy indicates the mixture of isomers.

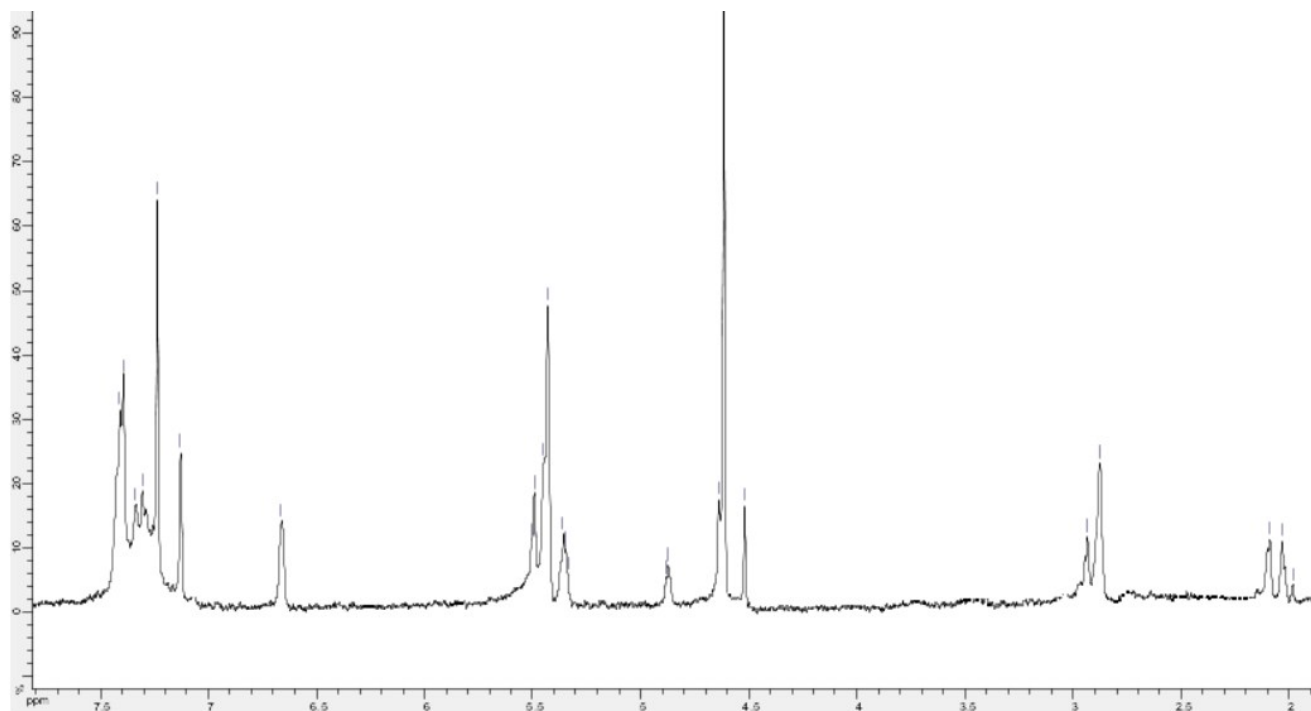


Figure S4: ^1H NMR (1D 1H), (CDCl_3 400 MHz): δ ppm: 7.41-7.31 (5H, CH of Ph), 7.13 and 6.66 (1H of triazole), 5.51-5.34 (2H of Ph-CH_2 and 2H of diene), 4.88-4.52 (5H of Cp free and 4H of Cp sub. when H^+ is added to Cp free), 2.93-2.88 (2H of diene), 2.09-2.04 (2H free).

Oxidation of benzylmethyl-(trz- η^4 -C₅H₅Co^ICp) giving back the cationic compound benzylmethyl(triazolyl)- η^5 -C₅H₄Co^{III}Cp (PF₆).

a) ESI-MS

Interestingly, upon recording the ESI-MS of benzylmethyl-(trz- η^4 -C₅H₅Co^ICp), the molecular peak of the cationic compound was observed. This method used a flow of methanol that reacted with the neutral compound (-trz η^4 -C₅H₅Co^ICp) to give back the starting material (-trz η^5 -C₅H₄Co^{III}Cp). It is believed that the hydride of benzylmethyl-(trz- η^4 -C₅H₅Co^ICp), is protonated by minute water amount in methanol to give molecular hydrogen⁵ and cobalticenium hydroxide.

ESI MS Spectrum:

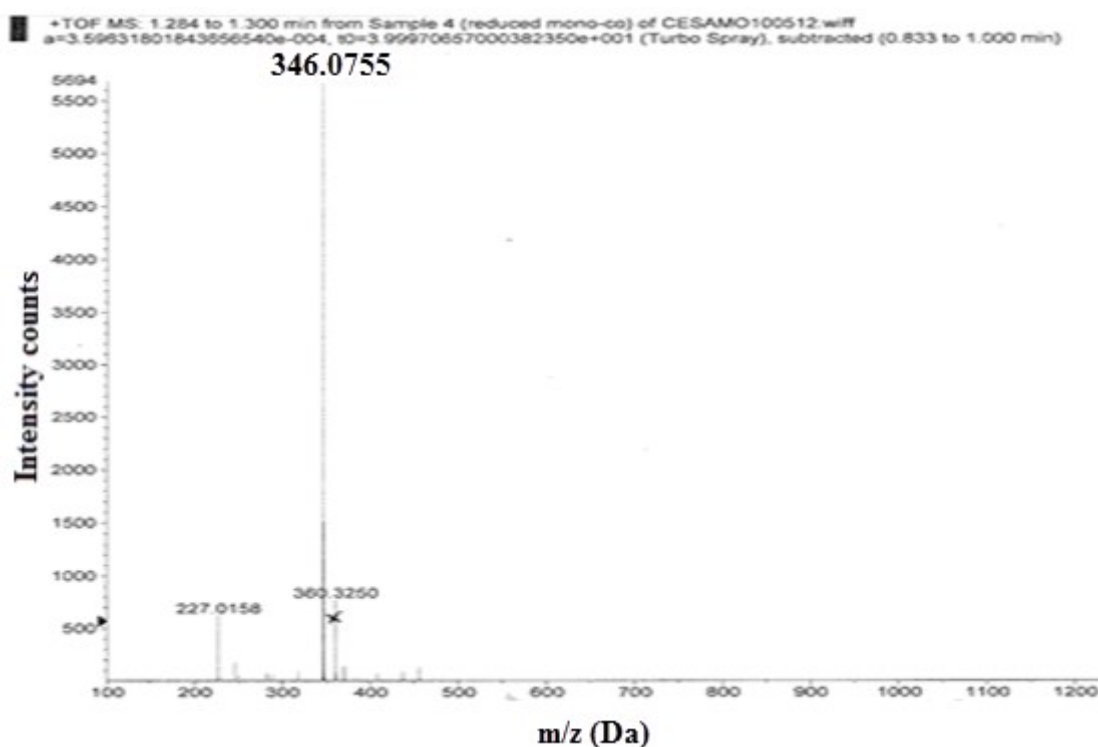


Figure S5: ESI MS(m/z): Calcd for C₁₉H₁₇N₃Co: 346.2916, Found: 346.0748.

The instrument is equipped with an ESI source, and spectra were recorded in the positive mode. The electrospray needle was maintained at 5000V and operated at room temperature. Samples were introduced by injection through a 20 μ L sample loop into a 4500 μ L/min flow of methanol from the LC pump.

b) CV after one night under air

Cyclic voltammetry also confirmed the oxidation of benzylmethyl-(trz- η^4 -C₅H₅Co^ICp), back to benzylmethyl(triazolyl)- η^5 -C₅H₄Co^{III}Cp(PF₆). The CV of benzylmethyl-(trz- η^4 -C₅H₅Co^ICp), was recorded in CH₂Cl₂ where two irreversible oxidation waves were found at 0.3 V and 0.65 V vs. [FeCp₂*]⁺⁰ (corresponding to the oxidation of triazolylcyclopentadiene-cobalt-Cp due to the preferential hydride reduction of the electron-poorer substituted ring and triazolylcyclopentadienyl-cobalt-cyclopentadiene respectively). After evaporating the solvent overnight under air, THF was added, and the CV was recorded again in which the two distinct reduction waves of cationic cobalticenium (PF₆) appeared. However, scanning towards the positive potentials the two oxidation waves of benzylmethyl-(trz- η^4 -C₅H₅Co^ICp), were not found indicating again the reoxidation of the neutral product to cationic benzylmethyl(triazolyl)- η^5 -C₅H₄Co^{III}Cp(PF₆) one and the reversibility of the system.

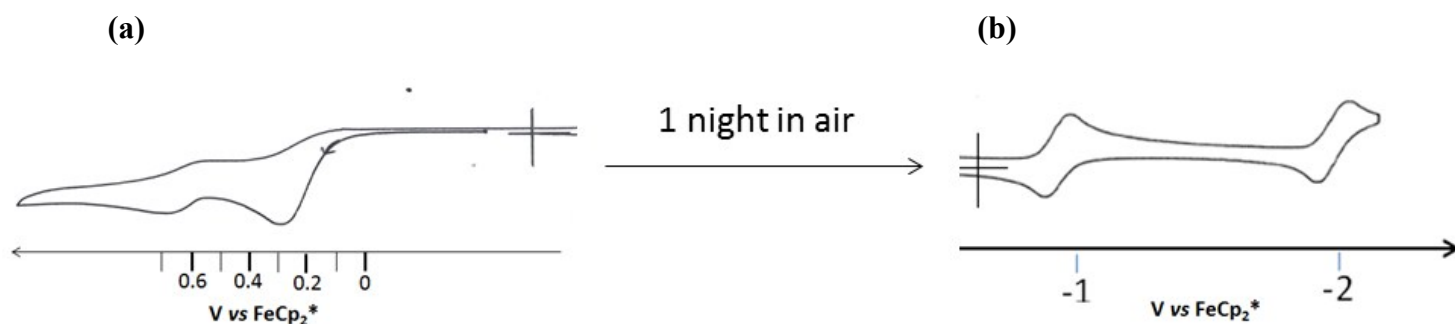


Figure S6: (a) CV in distilled CH₂Cl₂, (b) CV in THF after one night in air. Reference electrode : Ag ; working and counter electrodes : Pt ; scan rate: 0.2 V/s ; supporting electrolyte: [*n*-Bu₄N][PF₆].

Oxidation of benzylmethyl-(trz- η^4 -C₅H₅Co^ICp) with HCl

After these observations the oxidation experiment was conducted. benzylmethyl-(trz- η^4 -C₅H₅Co^ICp), in THF reacted with a diluted aqueous solution of 1.5 equiv. of HCl (aq.), and the color of the solution changed immediately from wine-red to light yellow (figure 1). The solvents were evaporated and the yellow sticky solid was all dissolved in H₂O showing that benzylmethyl(triazolyl)- η^5 -C₅H₄Co^{III}Cp(Cl) was formed, and that the reaction was quantitative (equation S2). ¹H NMR in D₂O showed all the corresponding proton peaks of benzylmethyl(triazolyl)- η^5 -C₅H₄Co^{III}Cp(Cl), whereas the UV-vis. spectrum showed the disappearance of the absorption bands at 410 nm and 530 nm and the appearance of the absorption bands of cationic triazolyl-cobalticenium.

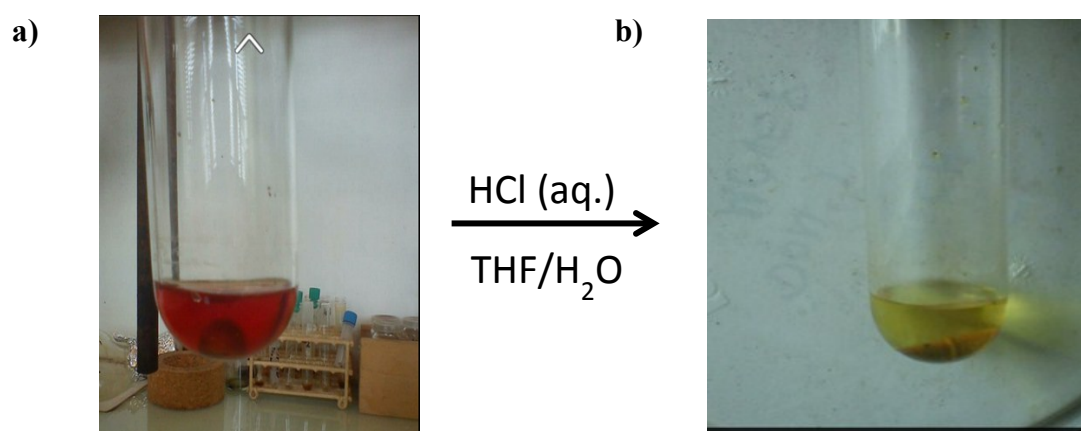


Figure S7: Photographs of a) benzylmethyl-(trz- η^4 -C₅H₅Co^ICp) and b) benzylmethyl(triazolyl)- η^5 -C₅H₄Co^{III}Cp(Cl) after addition of an aqueous HCl solution.

Experimental procedure for the synthesis of benzylmethyl(triazolyl)- η^5 -C₅H₄Co^{III}Cp(Cl)

Benzylmethyl-(trz- η^4 -C₅H₅Co^ICp) (15 mg, 0.04 mmol, 1 equiv.) was solubilized in 60 mL of THF. Then a 10 mL aqueous solution of HCl (0.05 mmol, 1.2 equiv.) was added dropwise, and the color gradually changed from deep red to light yellow giving back the cationic product **benzylmethyl(triazolyl)- η^5 -C₅H₄Co^{III}Cp(Cl)** and molecular hydrogen. After stirring for 10 min. the mixture of solvents was evaporated. Solubilization in water, filtration and evaporation of the solvent gave **benzylmethyl(triazolyl)- η^5 -C₅H₄Co^{III}Cp(Cl)** as a yellow waxy product in quantitative yield (14 mg). ¹H NMR (1D 1H), (D₂O, 400 MHz): δ ppm: 8.45 (1H, CH of triazole), 7.47 (5H, CH of Ar), 6.25 (2H, CH of Cp sub.), 5.88 (2H, CH of Cp sub.), 5.70 (2H, Ar-CH₂), 5.60 (5H, Cp free). UV-vis.: $\lambda_{\text{max}1}$ = 350 nm, $\lambda_{\text{max}2}$ = 410 nm.

^1H NMR of benzylmethyl(triazolyl)- $\eta^5\text{-C}_5\text{H}_4\text{Co}^{\text{III}}\text{Cp}(\text{Cl})$

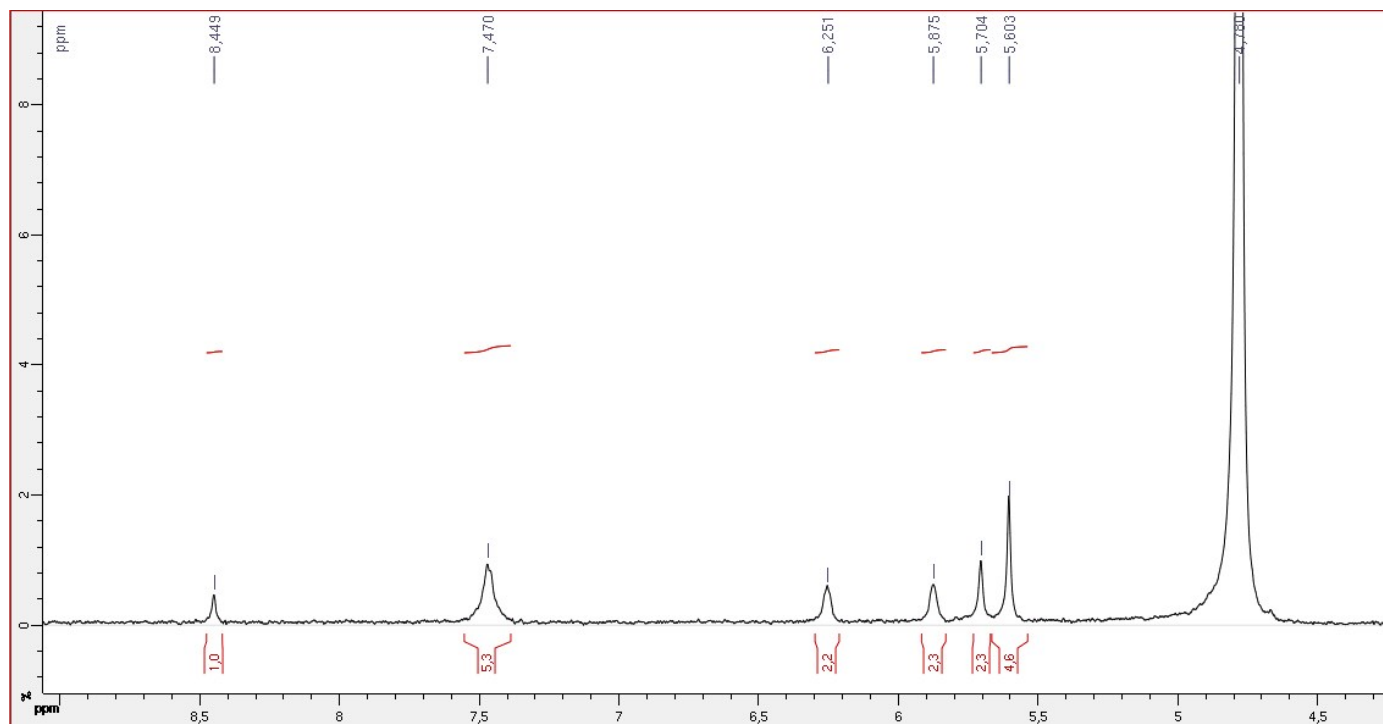


Figure S8: ^1H NMR (1D 1H), (D_2O , 400 MHz): δ ppm: 8.45 (1H, CH of triazole), 7.47 (5H, CH of Ar), 6.25 (2H, CH of Cp sub.), 5.88 (2H, CH of Cp sub.), 5.70 (2H, Ar-CH₂), 5.60 (5H, Cp free).

UV-visible spectrum of benzylmethyl(triazolyl)- η^5 -C₅H₄Co^{III}Cp(Cl)

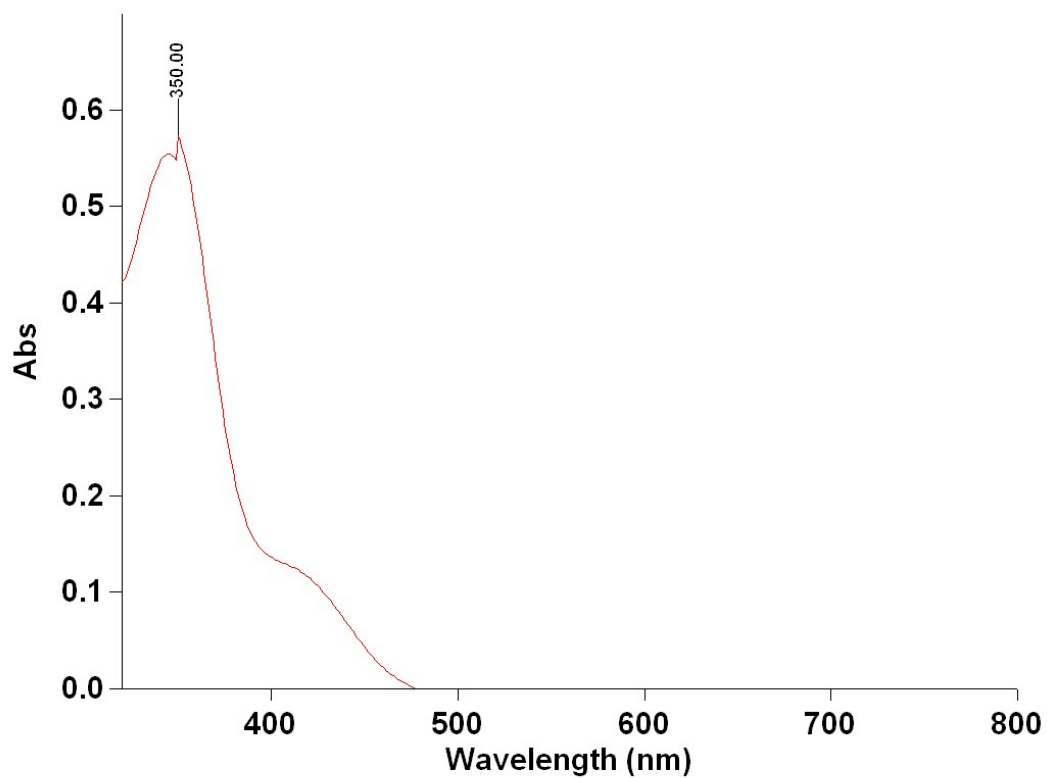


Figure S9: Observation of an absorption band at $\lambda_{\text{max}_1} = 350 \text{ nm}$ and an absorption shoulder at $\lambda_{\text{max}_2} = 410 \text{ nm}$ corresponding to benzylmethyl(triazolyl)- η^5 -C₅H₄Co^{III}Cp (Cl) product.

Formation of molecular hydrogen during oxidation of benzylmethyl-(trz- η^4 -C₅H₅Co^ICp).

The oxidation reaction was repeated in a sealed NMR tube in which benzylmethyl-(trz- η^4 -C₅H₅Co^ICp) was solubilized in deuterated THF; 1.1 equiv. of HPF₆(aq.) was added into the tube (equation S3). The color changed from red to orange instantaneously and the ¹H NMR spectrum was recorded. Except of the typical proton peaks of benzylmethyl(triazolyl)- η^5 -C₅H₄Co^{III}Cp(PF₆) formed and the disappearance of the proton peaks of the product benzylmethyl-(trz- η^4 -C₅H₅Co^ICp), a new proton peak at 4.6 ppm was observed and assigned to H₂.

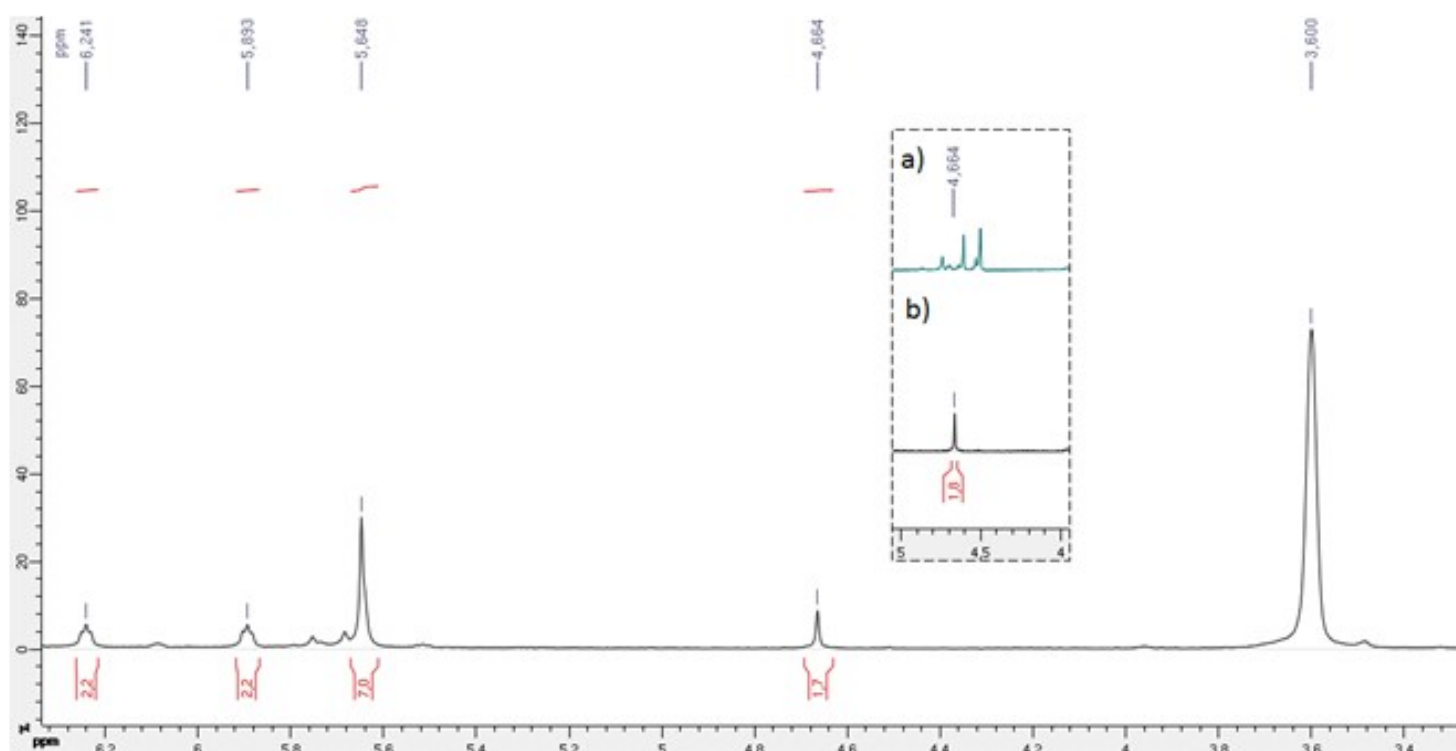
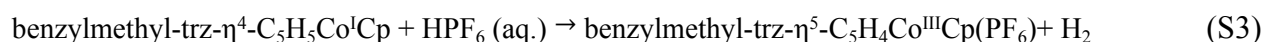
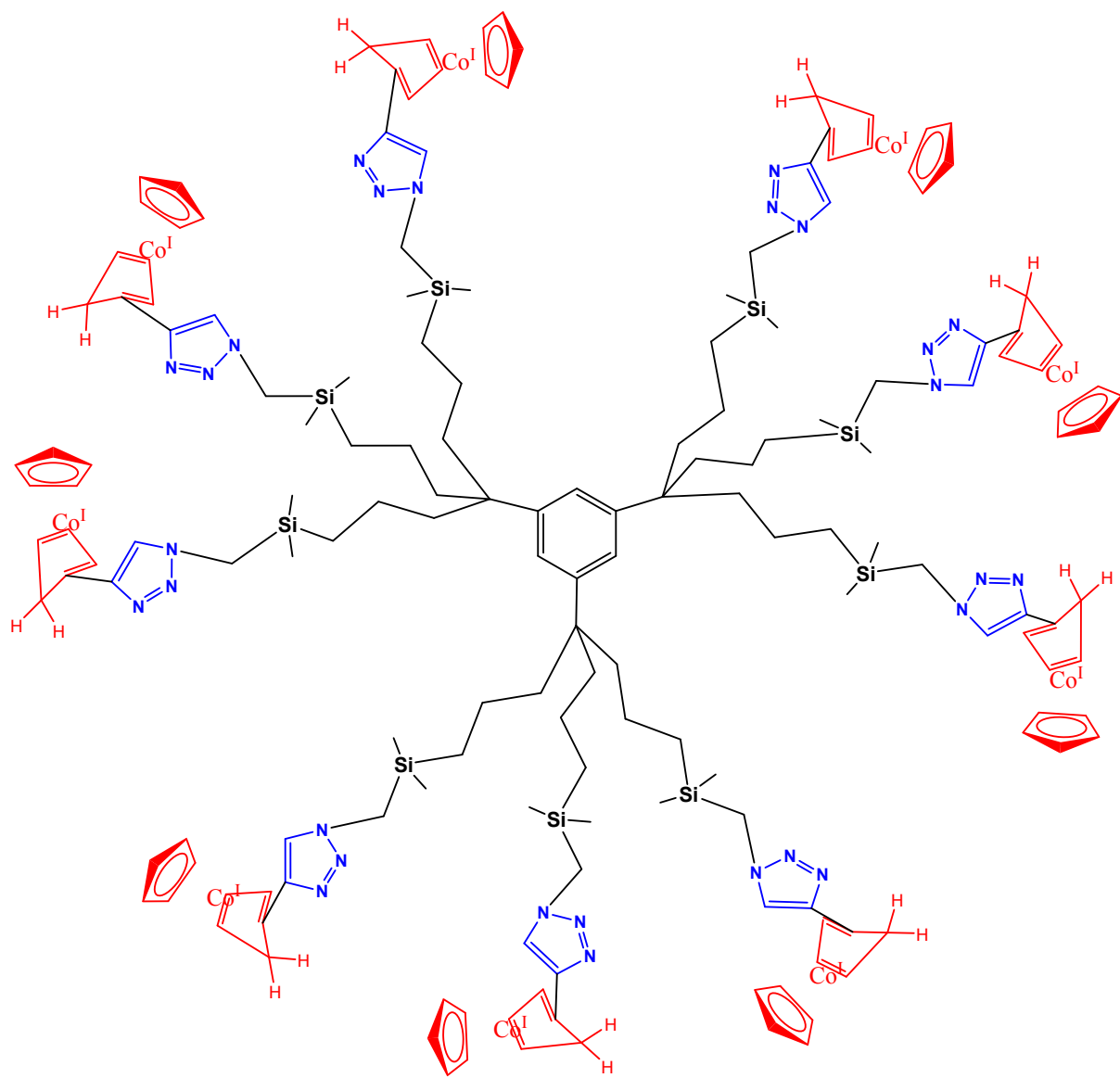


Figure S10: ¹H NMR (1D 1H), (THF, 300 MHz): In situ oxidation of benzylmethyl(triazolyl)- η^5 -C₅H₄Co^IC₅H₆ in a sealed NMR tube by addition of HPF₆. The proton peak at 4.66 ppm corresponds to the hydrogen produced.

In the zoom is shown a) the area 5.0-4.0 ppm before the addition of HPF₆ and b) after the addition of HPF₆.

Dendrimer filled DHR 4 (G₀)



FigureS11: Structure of filled DHR 4. A single isomer is represented for each branch; for the structures of the four isomer structures, see Figure S1. For 9 branches, there are 36 possible isomers.

Experimental procedure for DHR 4

The empty DHR **1** (PF_6)² (solid, 20 mg, 0.004 mmol, 1 equiv.) reacted with solid NaBH_4 (2 mg, 0.06 mmol, 13.5 equiv.) in distilled THF (30 mL) for 20 min at 0°C under N_2 . The color of the solution changed from light yellow to deep red. Then, the solution was filtered under nitrogen. The solvent was evaporated *in vacuo*. The deep red solid was washed three times with 15 mL of distilled H_2O . The filled DHR **4** was obtained as a deep red powder in quantitative yield (13 mg). ¹H NMR (1D, 1H), (CD_3CN , 400 MHz) of **4**: δ_{ppm} : 7.00, 6.83 and 6.51 (9H, CH of trz and 3H, CH of arom.core), 5.93-5.15 (18H of diene), 4.69-4.48 (45H of free Cp and 36H of substituted Cp when H^- is added to free Cp), 4.34 (18H, SiCH_2 -trz), 3.18-2.91 (18H of diene), 2.33-2.04 (18H free), 1.61 (18H, $\text{CH}_2\text{CH}_2\text{CH}_2\text{Si}$), 1.23 (18H, $\text{CH}_2\text{CH}_2\text{CH}_2\text{Si}$), 0.54 (18H, 18H, $\text{CH}_2\text{CH}_2\text{CH}_2\text{Si}$), -0.05 (54H, $\text{Si}(\text{CH}_3)_2$). ¹³C NMR (1D, 1H), (CD_3COCD_3 , 100 MHz) of **4**: δ_{ppm} : 150.62 (*Cq* of arom.core), 148.41 and 147.82 (*Cq* of trz), 127.57 and 121.83 (CH of trz), 124.28 (CH of arom.core), 80.02-72.96 (CH of Cp free, CH of Cp sub., *Cq* of Cp sub. and CH of diene), 48.48-39.81 (*CqCH}_2\text{CH}_2\text{CH}_2\text{Si}, *CqCH}_2\text{CH}_2\text{CH}_2\text{Si}, trz- CH_2Si , CH of diene and CH_2 of Cp), 19.51-15.53 (*CqCH}_2\text{CH}_2\text{CH}_2\text{Si} and *CqCH}_2\text{CH}_2\text{CH}_2\text{Si}), -3.62 ($\text{Si}(\text{CH}_3)_2$). UV-vis.: $\lambda_{\text{max}1} = 410$ nm, $\lambda_{\text{max}2} = 537$ nm. ESI MS of **4** ($\text{C}_{171}\text{H}_{223}\text{Si}_9\text{N}_{27}\text{Co}_9(\text{OH})_3$): calc. 3490.0 Da; found. 3491.0 Da.****

UV-visible spectrum of DHR 4

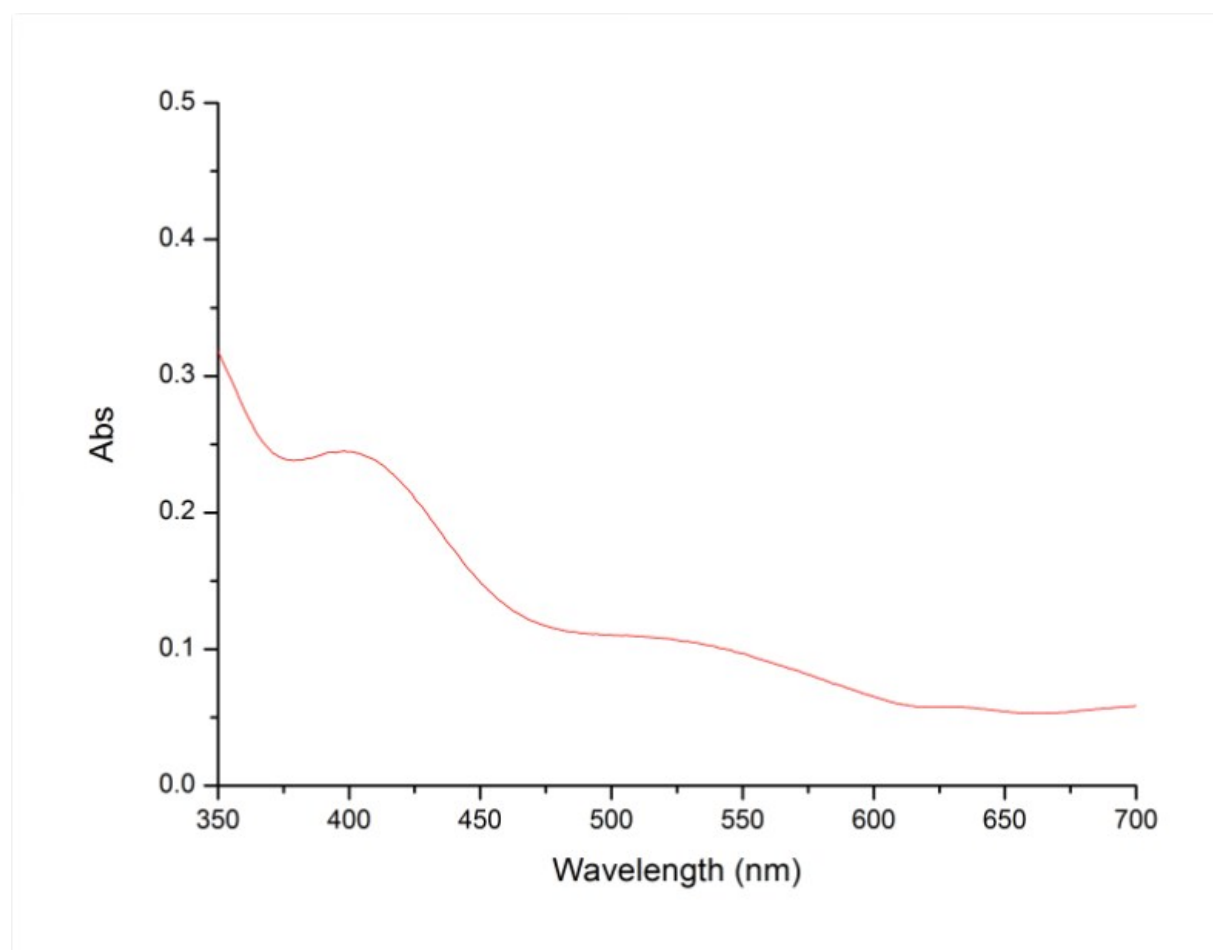


Figure S12: An absorption band is observed at $\lambda_{\max_1} = 410$ nm and an absorption shoulder appears at $\lambda_{\max_2} = 537$ nm corresponding to the product 4.

IR (KBr) of DHR 4

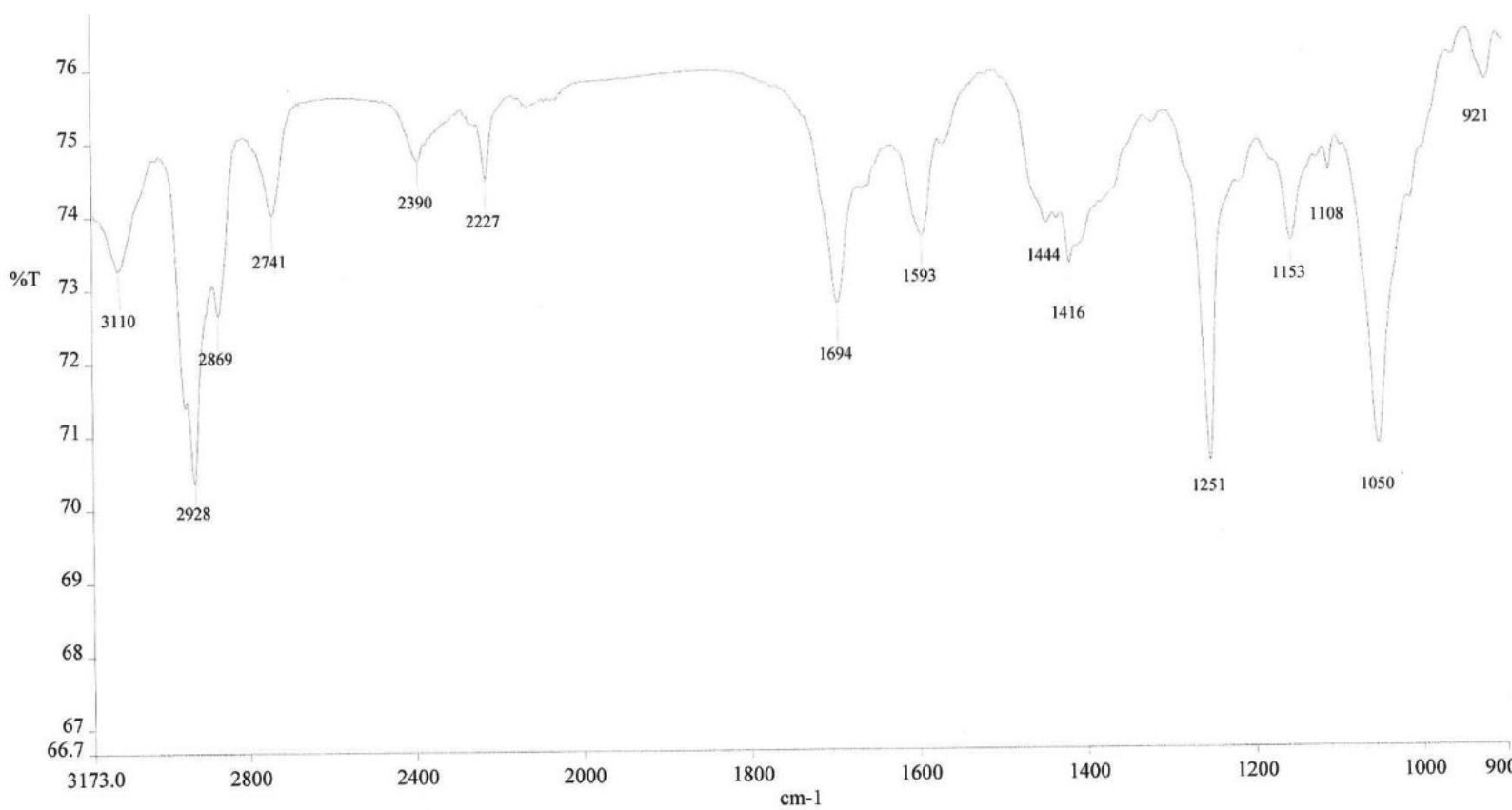


Figure S13: IR(KBr) of 4: 3110, 2928, 2869, 2741, 1694, 1251, 1153, 1050 (cm⁻¹).

ESI MS of 4

- The method has a limit of 2000 m/z Da for the molar mass, m being the mass and z the charge. When the mass is large, the product is found within this limit, in a form of 'monocharged' fragments ($z = 1$) or 'dicharged' entities ($z = 2$). The actual mass m is calculated as: $M = m/z$, i.e. the double of the m/z peak. For the molecular peak, the calculated M value is 3490.0 Da that is observed below as major peaks at 1745.0 and 1745.5 as expected corresponding to 3490.0 Da and 3491.0 Da respectively, fully conforming the DHR structure of **4**.

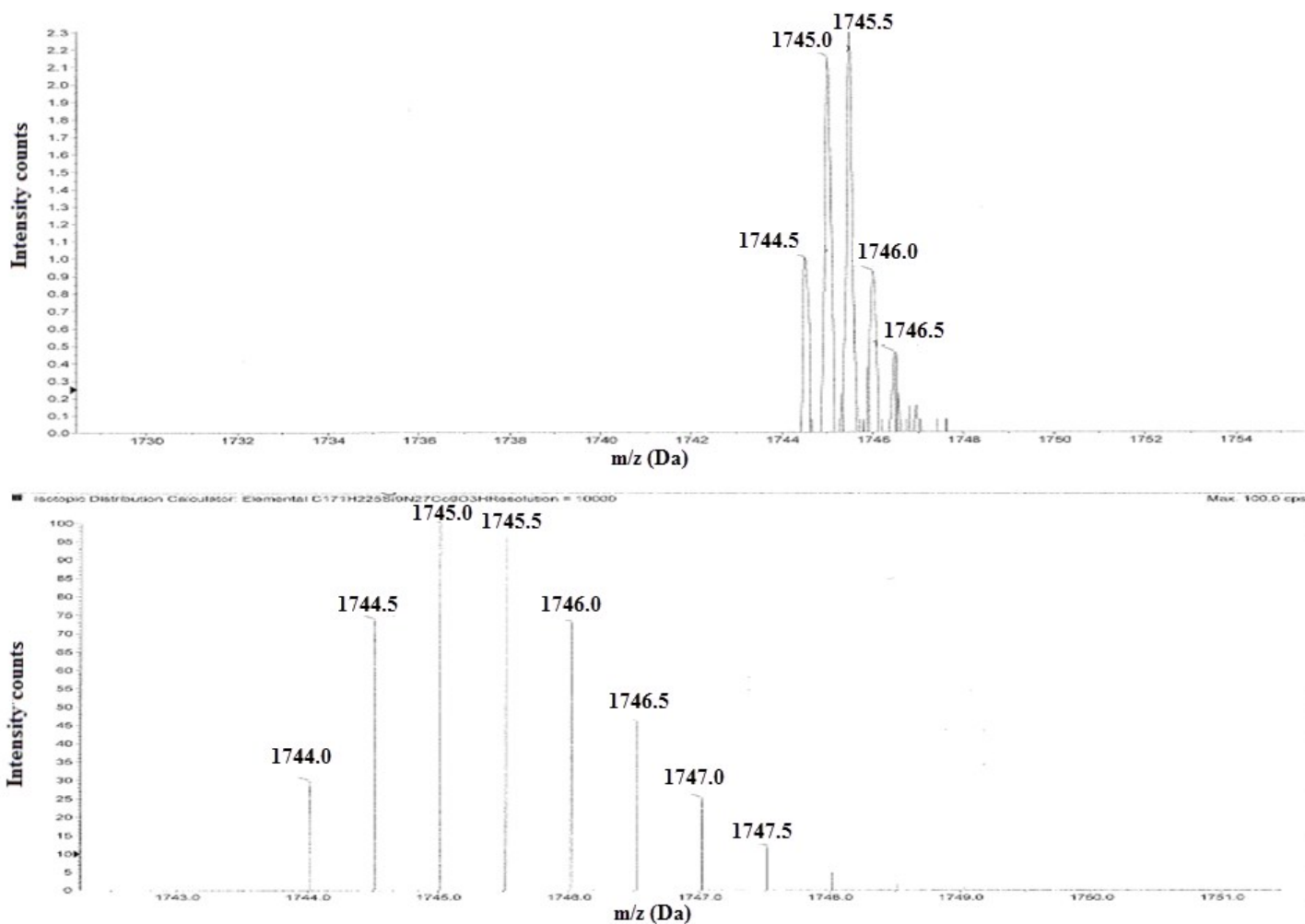


Figure S14: ESI MS of **4** ($C_{171}H_{223}Si_9N_{27}Co_9(OH)_3$): calc. 3490.0 Da; found. 3491.0 Da

AFM of DHR 4

AFM microscopy of **4** (packages of several dendrimers together) shows the average height on the mica surface of $h = 0.45$ nm (presenting another bilayer at $h' = 1.2$ nm due to the small size of dendrimer **4**). The following generations (G_1 and G_2) present this phenomenon to a much lesser extent.

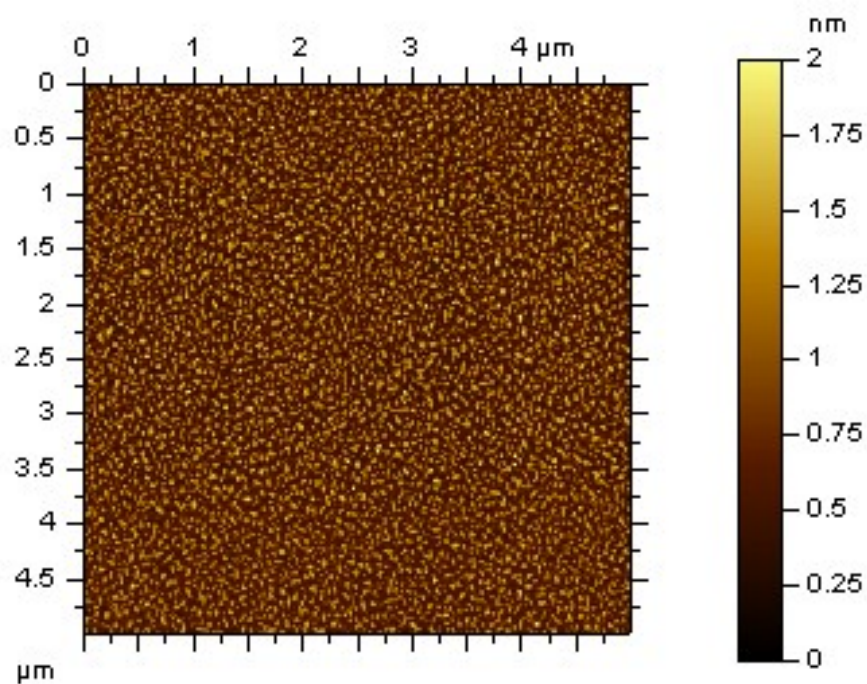


Figure S15: AFM topography image of **4 on a mica surface.**

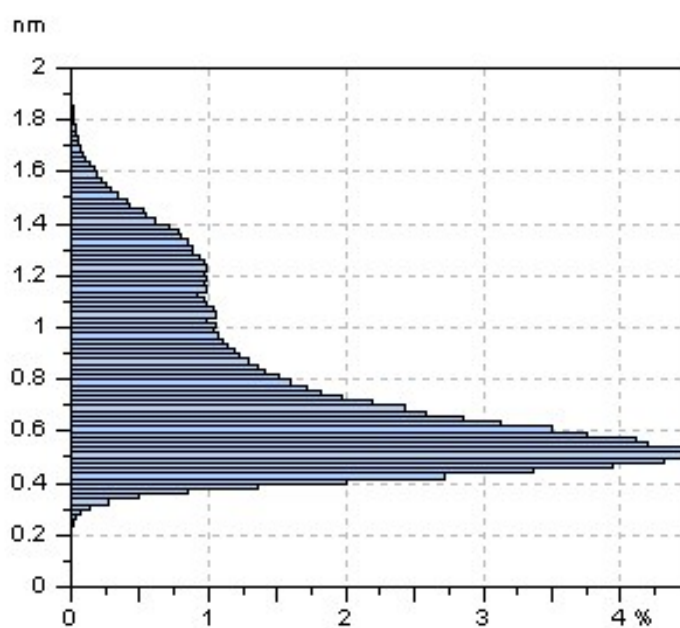


Figure S16: Statistical height distribution of 4.

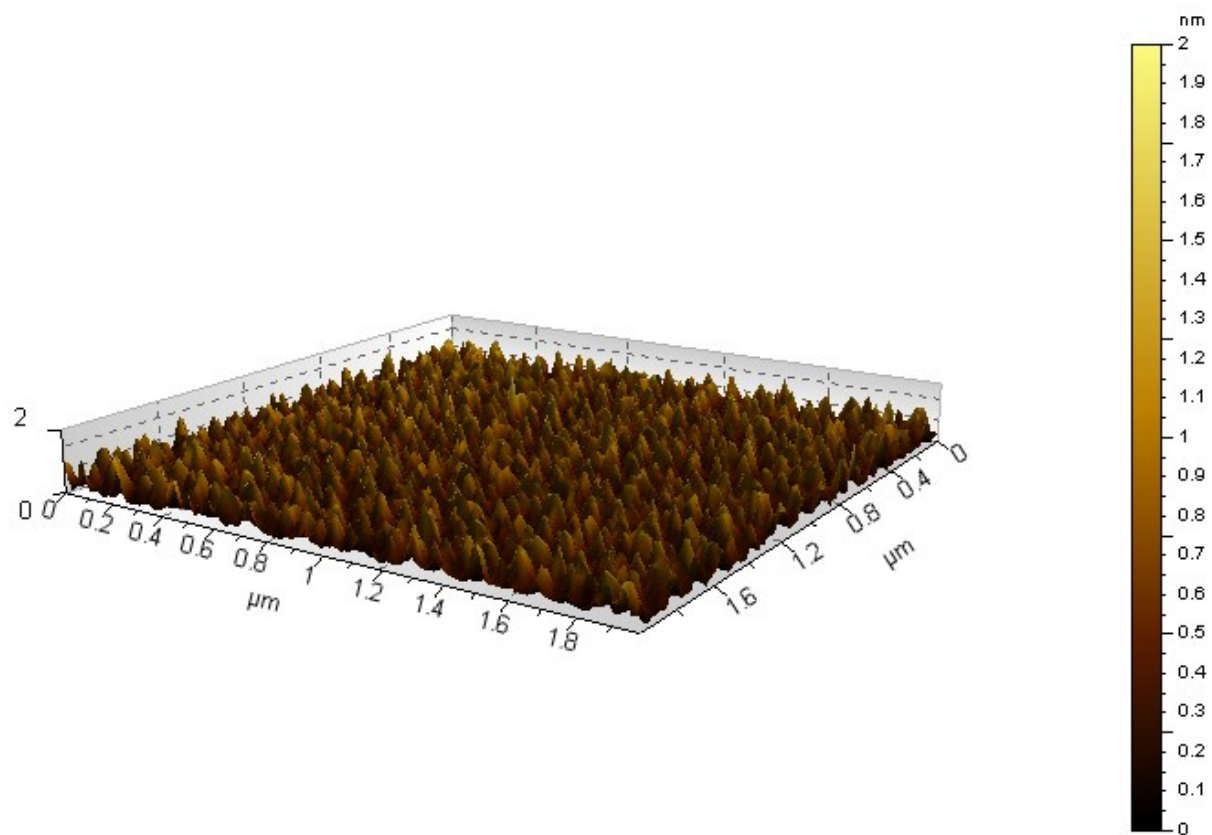


Figure S17: 3D AFM topography image

¹H NMR of DHR 4

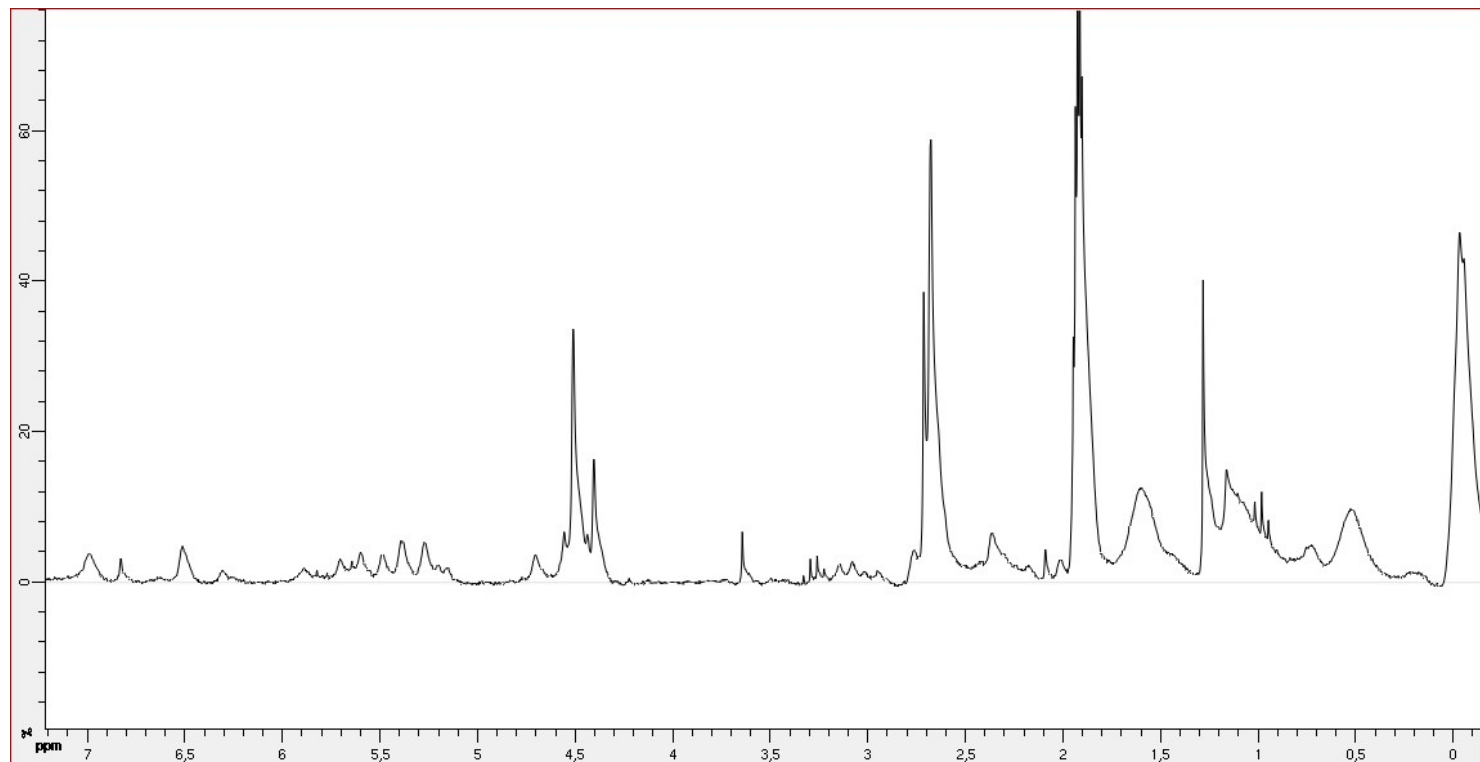


Figure S18: ¹H NMR (1D, 1H), (CD₃CN, 400 MHz) of **4**: δ_{ppm} : 7.00, 6.83 and 6.51 (9H, CH of trz and 3H, CH of arom.core), 5.93-5.15 (18H of diene), 4.69-4.48 (45H of free Cp and 36H of substituted Cp when H⁻ is added to free Cp), 4.34 (18H, SiCH₂-trz), 3.18-2.91 (18H of diene), 2.33-2.04 (18H free), 1.61 (18H, CH₂CH₂CH₂Si), 1.23 (18H, CH₂CH₂CH₂Si), 0.54 (18H, 18H, CH₂CH₂CH₂Si), -0.05 (54H, Si(CH₃)₂).

^{13}C NMR of DHR 4

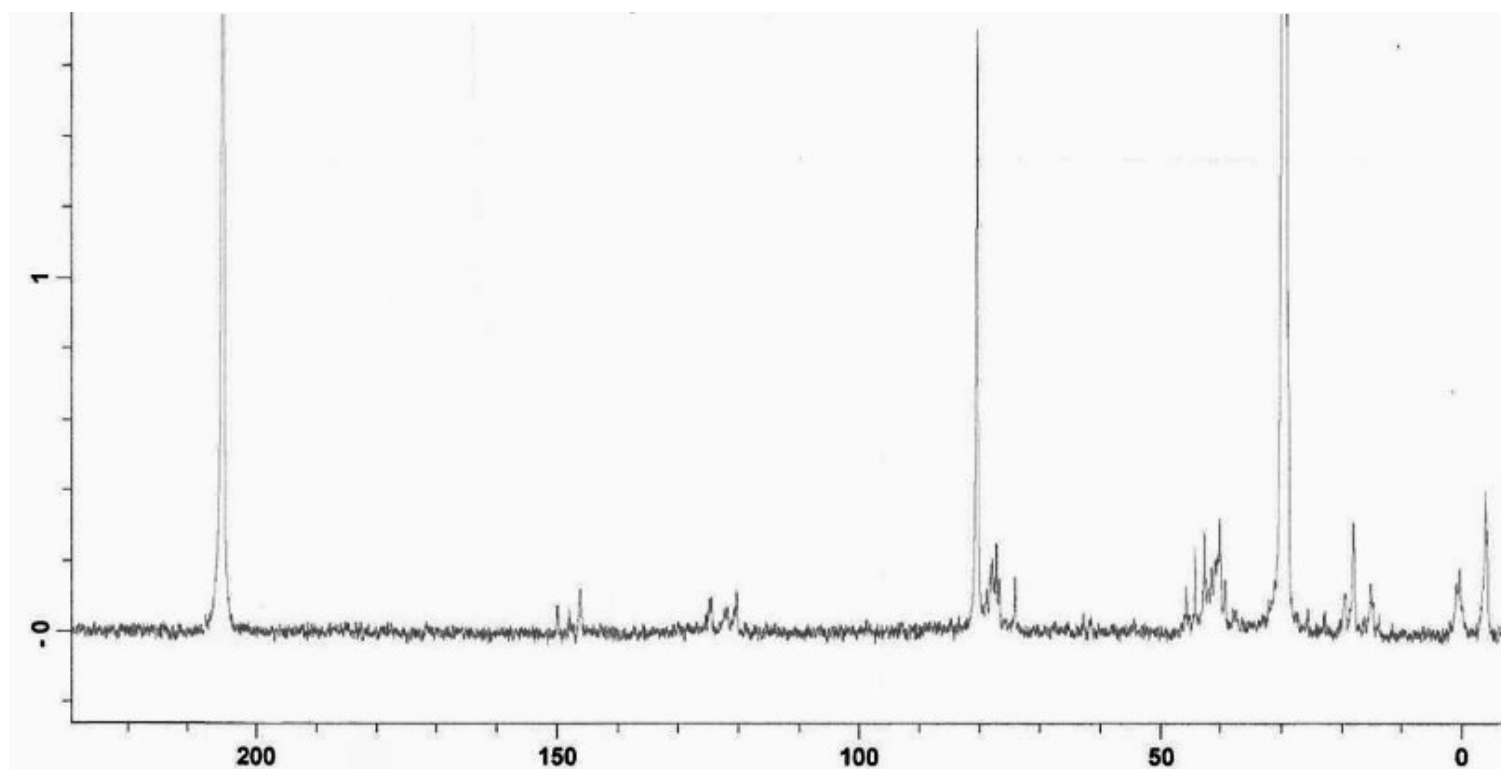


Figure S19: ^{13}C NMR (1D, 1H), (CD_3COCD_3 , 100 MHz) of **4**: δ_{ppm} : 150.62 (C_q of arom.core), 148.41 and 147.82 (C_q of trz), 127.57 and 121.83 (CH of trz), 124.28 (CH of arom.core), 80.02-72.96 (CH of Cp free, CH of Cp sub., C_q of Cp sub. and CH of diene), 48.48-39.81 ($C_q\text{CH}_2\text{CH}_2\text{CH}_2\text{Si}$, $C_q\text{CH}_2\text{CH}_2\text{CH}_2\text{Si}$, trz- CH_2Si , CH of diene and CH_2 of Cp), 19.51-15.53 ($C_q\text{CH}_2\text{CH}_2\text{CH}_2\text{Si}$ and $C_q\text{CH}_2\text{CH}_2\text{CH}_2\text{Si}$), -3.62 ($\text{Si}(\text{CH}_3)_2$).

HSQC 2D NMR spectroscopy of DHR 4

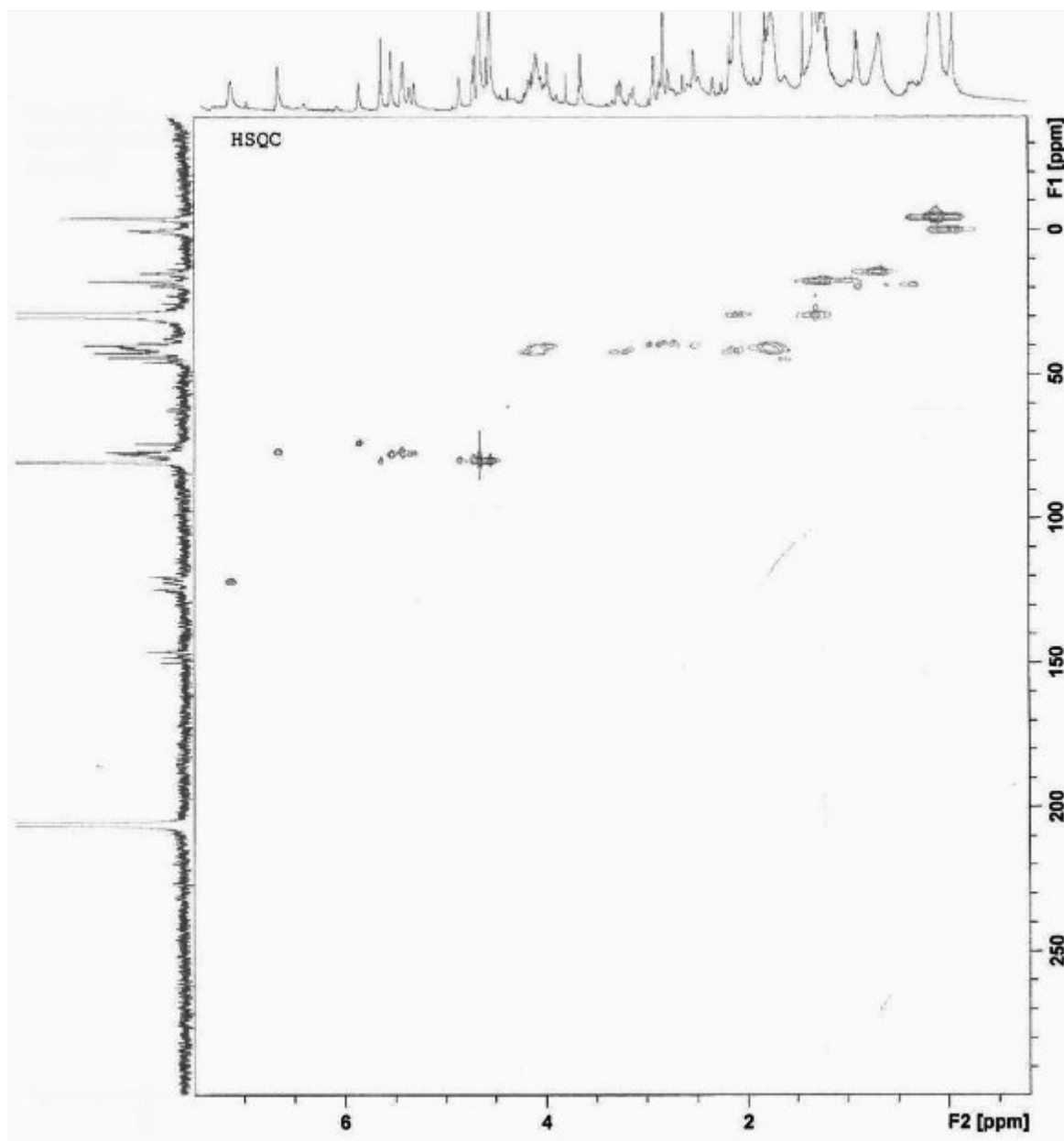


Figure S20: HSQC 2D NMR spectrum of **4**.

Dendrimer filled DHR 5 (G_1)

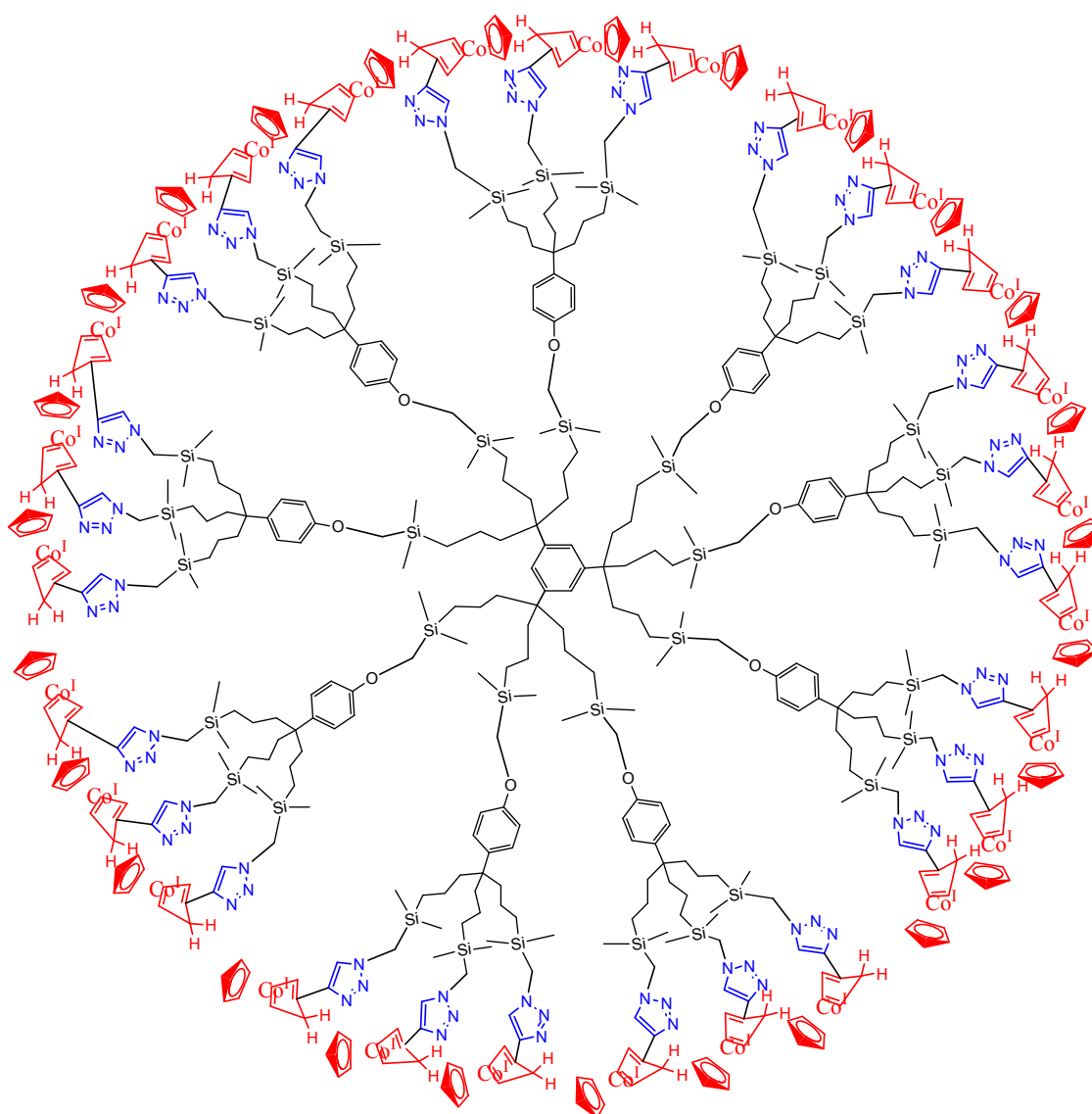


Figure S21: Structure of filled DHR 5. A single isomer is represented on each branch. For the 4 possible isomers on each branch, see Figure S1. With 27 branches, there are 108 possible isomers.

Experimental procedure for 5

The empty DHR **2**(PF₆) solid (25 mg, 0.002 mmol, 1 equiv.) reacted with NaBH₄ (3 mg, 0.08 mmol, 40.5 equiv.) in distilled THF (20 mL) for 20 min at 0°C under N₂. The color of the solution changed from colorless to deep red. Then, the solution was filtered under nitrogen. The solvent was evaporated *in vacuo*. The deep red solid was washed three times with 10 mL of distilled H₂O. The filled DHR **5** was obtained as a deep red powder in quantitative yield (21 mg). ¹H NMR (1D, 1H), (CD₃COCD₃, 400 MHz) of **5**: δ_{ppm}: 7.20, 7.05 6.92 and 6.63 (27H, CH of trz and 39H, CH of arom.core), 5.84-5.31 (54H of diene), 4.94-4.72 (135H of free Cp and 108H of substituted Cp when H⁻ is added to free Cp), 4.53 (54H, SiCH₂-trz), 3.38 (18H, SiCH₂O) 3.25-2.84 (54H of diene), 2.50-2.02 (54H free), 1.69 (72H, CH₂CH₂CH₂Si), 1.22 (72H, CH₂CH₂CH₂Si), 0.65 (72H, 18H, CH₂CH₂CH₂Si), 0.06 (216H, Si(CH₃)₂). ¹³C NMR (1D, 1H), (CD₃COCD₃, 75 MHz) of **5**: δ_{ppm}: 160.05 (arom. OCq), 139.95 and 134.83 (Cq of trz and Cq of aromatic core), 129.48-125.32 (CH of trz and CH aromatic), 81.96-78.30 (CH of Cp free, CH of Cp sub., Cq of Cp sub. and CH of diene), 68.10 (CH₂OAr), 49.87-41.73 (CqCH₂CH₂CH₂Si, CqCH₂CH₂CH₂Si, trz-CH₂Si, CH of diene and CH₂ of Cp), 24.34-15.21 (CqCH₂CH₂CH₂Si and CqCH₂CH₂CH₂Si), -5.88 (Si(CH₃)₂). UV-vis.: λ_{max1} = 415 nm, λ_{max2} = 527 nm.

UV-visible spectrum of DHR 5

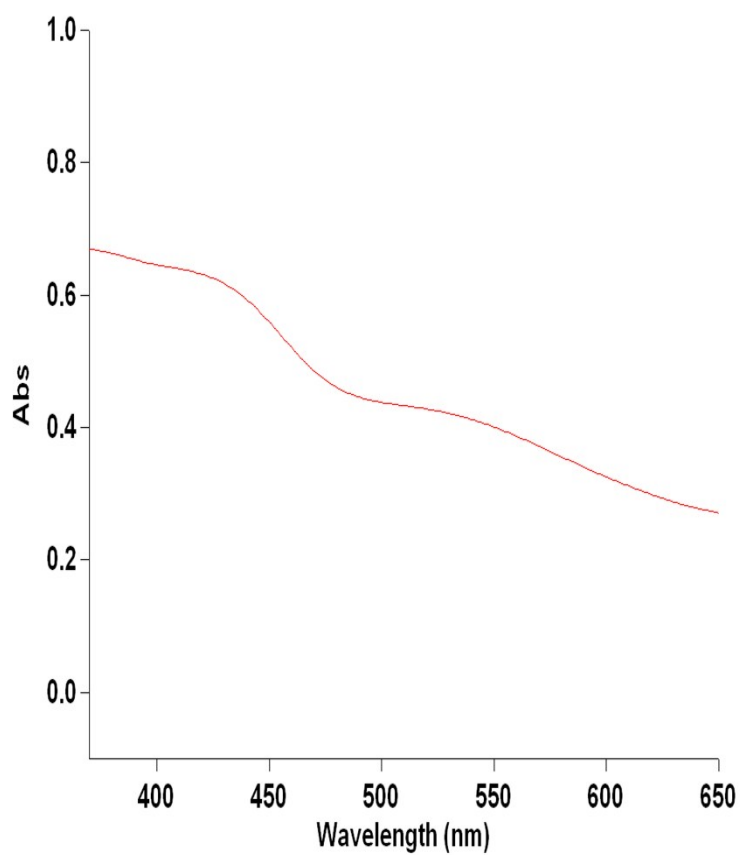


Figure S22: An absorption shoulder is observed at $\lambda_{\text{max}_1} = 415$ nm and an absorption shoulder appears at $\lambda_{\text{max}_2} = 527$ nm corresponding to the product **5**.

IR (KBr) of DHR 5

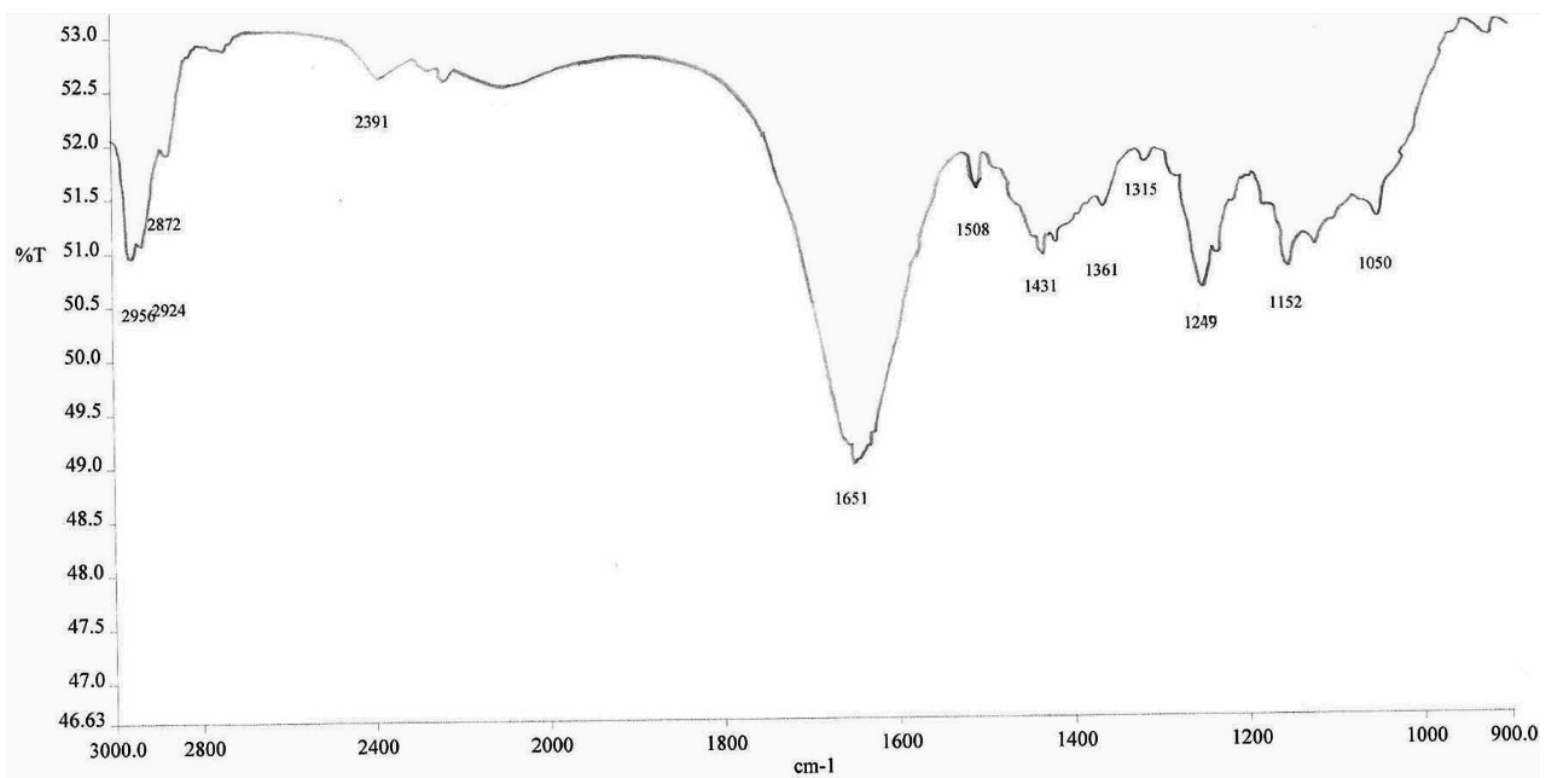


Figure S23: IR (KBr) of **5**: 3100, 2956, 2924, 2872, 1651, 1249, 1152, 1050 (cm⁻¹).

AFM studies of DHR 5

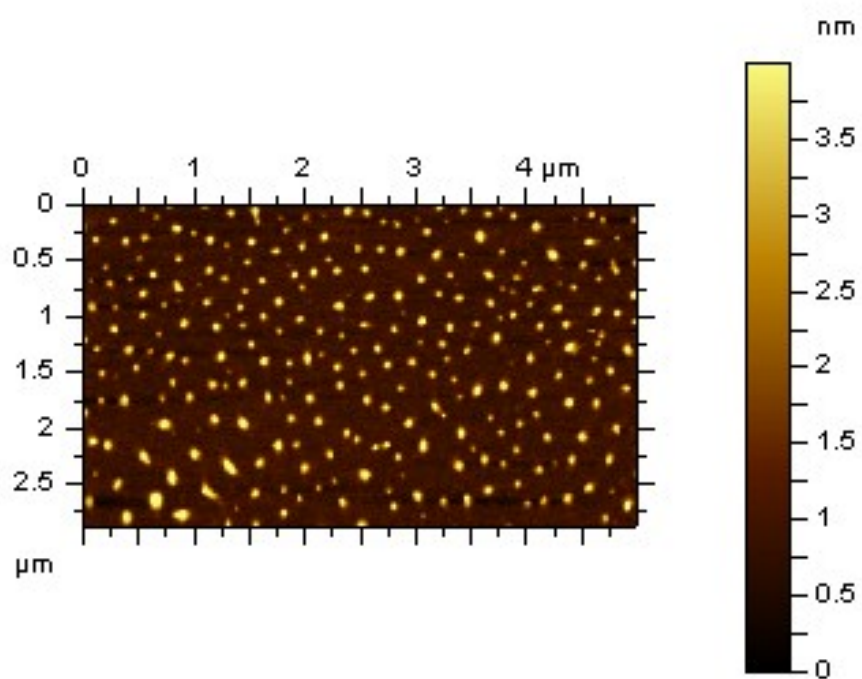


Figure S24: AFM topography image of **5** on a mica surface.

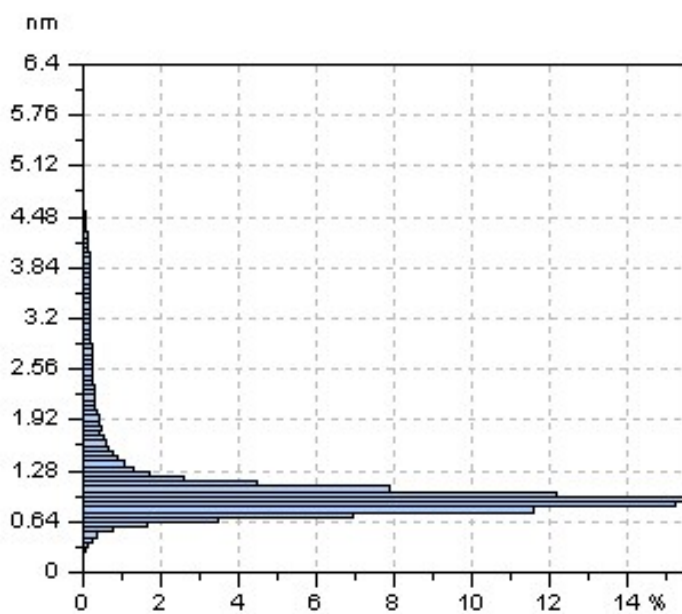


Figure S25: Statistical height distribution of **5**.

^1H NMR of DHR 5

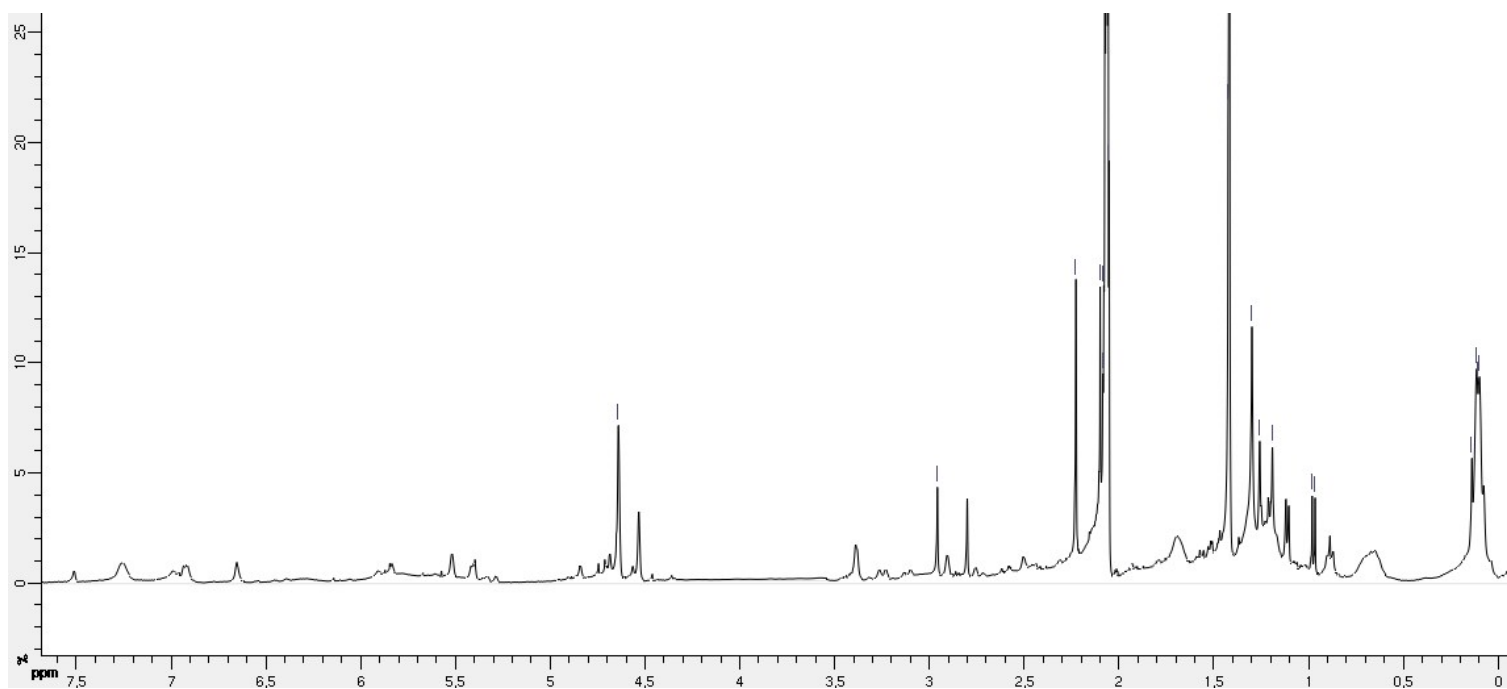


Figure S26: ^1H NMR (1D, 1H), (CD_3COCD_3 , 400 MHz) of **5**: δ_{ppm} : 7.20, 7.05 6.92 and 6.63 (27H, CH of trz and 39H, CH of arom.core), 5.84-5.31 (54H of diene), 4.94-4.72 (135H of free Cp and 108H of substituted Cp when H^- is added to free Cp), 4.53 (54H, $\text{SiCH}_2\text{-trz}$), 3.38 (18H, SiCH_2O) 3.25-2.84 (54H of diene), 2.50-2.02 (54H free), 1.69 (72H, $\text{CH}_2\text{CH}_2\text{CH}_2\text{Si}$), 1.22 (72H, $\text{CH}_2\text{CH}_2\text{CH}_2\text{Si}$), 0.65 (72H, 18H, $\text{CH}_2\text{CH}_2\text{CH}_2\text{Si}$), 0.06 (216H, $\text{Si}(\text{CH}_3)_2$).

^{13}C NMR of DHR 5

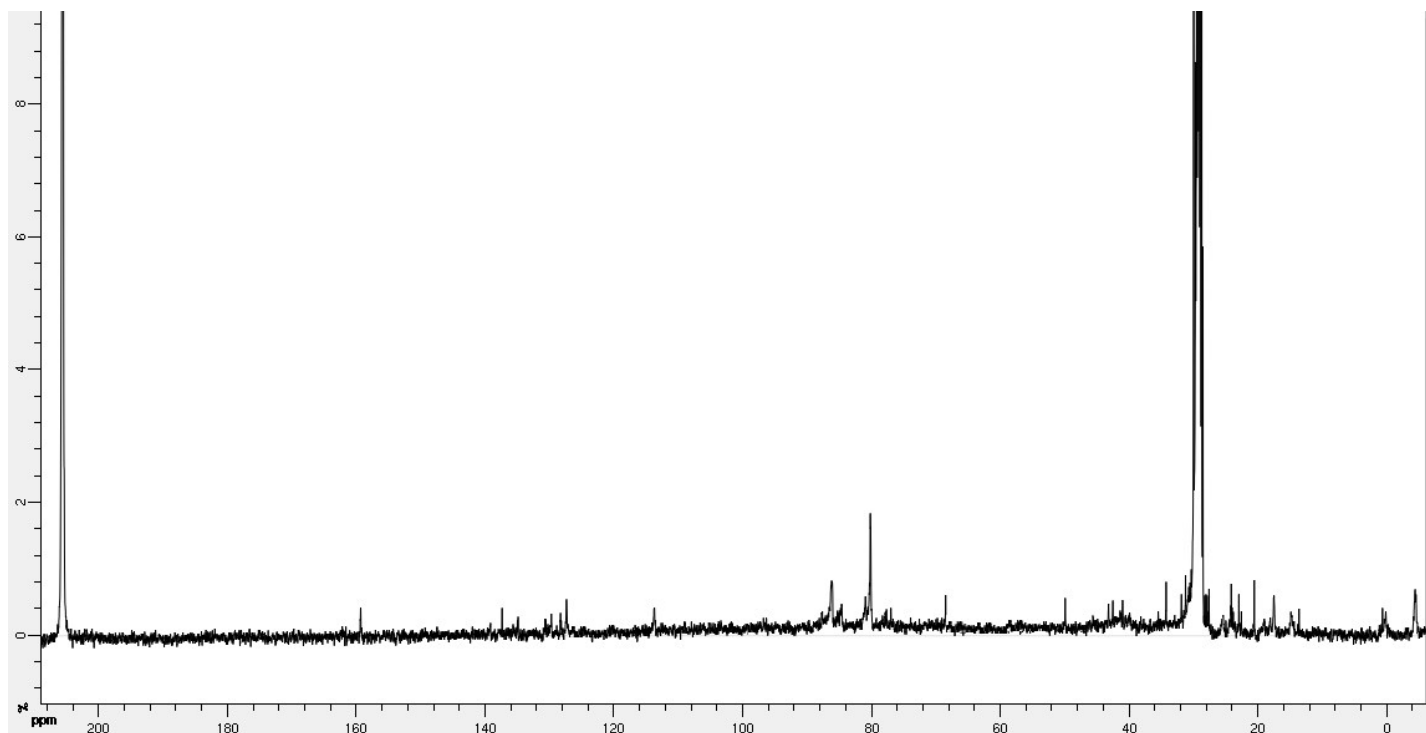


Figure S27: ^{13}C NMR (1D, 1H), (CD_3COCD_3 , 100 MHz) of **5**: δ_{ppm} : 160.05 (arom. OCq), 139.95 and 134.83 (Cq of trz and Cq of aromatic core), 129.48-125.32 (CH of trz and CH aromatic), 81.96-78.30 (CH of Cp free, CH of Cp sub., Cq of Cp sub. and CH of diene), 68.10 (CH_2OAr), 49.87-41.73 (Cq $\text{CH}_2\text{CH}_2\text{CH}_2\text{Si}$, Cq $\text{CH}_2\text{CH}_2\text{CH}_2\text{Si}$, trz- CH_2Si , CH of diene and CH_2 of Cp), 24.34-15.21 (Cq $\text{CH}_2\text{CH}_2\text{CH}_2\text{Si}$ and Cq $\text{CH}_2\text{CH}_2\text{CH}_2\text{Si}$), -5.88 ($\text{Si}(\text{CH}_3)_2$).

HSQC 2D NMR spectroscopy of DHR 5

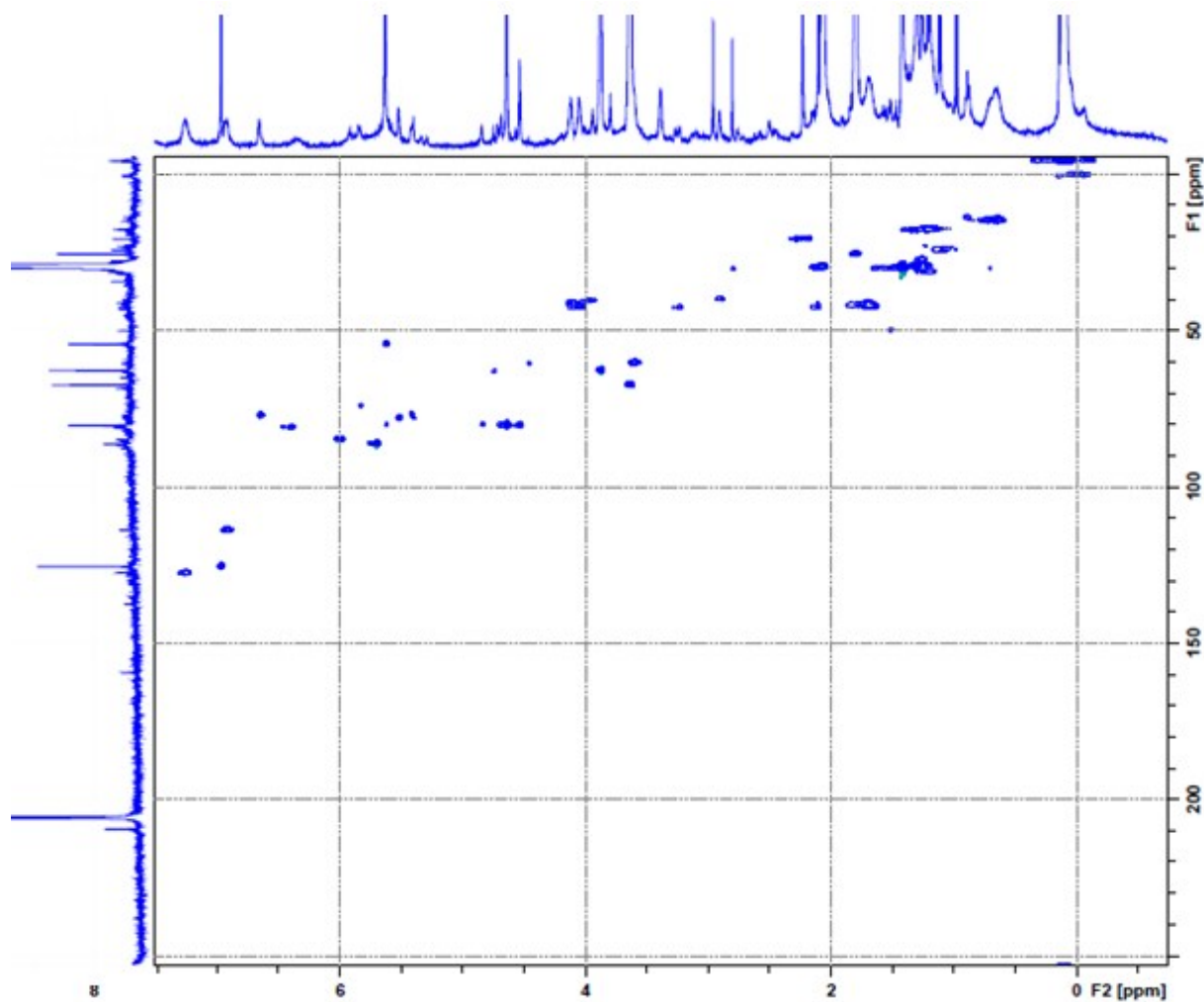


Figure S28: HSQC 2D NMR spectrum of **5**.

Dendrimer filled DHR 6

Experimental procedure for 6

The empty DHR **3**(PF₆) solid (20 mg, 0.4 x 10⁻³ mmol, 1 equiv.) reacted with NaBH₄ (1.9 mg, 0.05 mmol, 121.5 equiv.) in distilled THF (20 mL) for 20 min at 0°C under N₂. The color of the solution changed from colorless to deep red. Then, the solution was filtered under nitrogen. The solvent was evaporated *in vacuo*. The deep red solid was washed three times with 10 mL of distilled H₂O. The filled DHR **6** was obtained as a deep red powder in quantitative yield (14 mg). UV-vis.: $\lambda_{\text{max}1} = 408$ nm, $\lambda_{\text{max}2} = 524$ nm.

AFM studies of DHR **6**

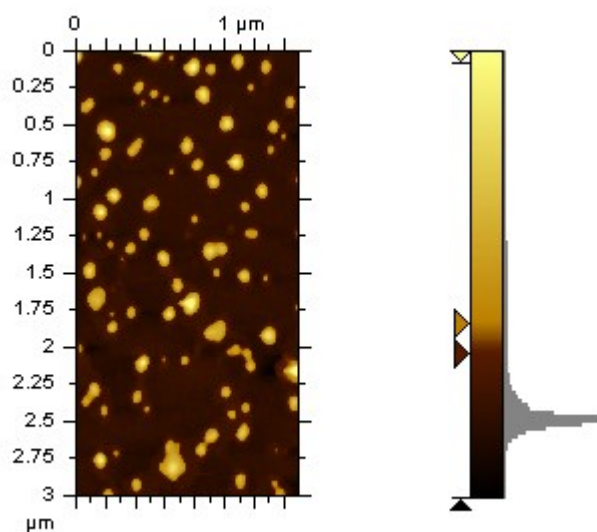


Figure S29: AFM topography image of **6** on a mica surface.

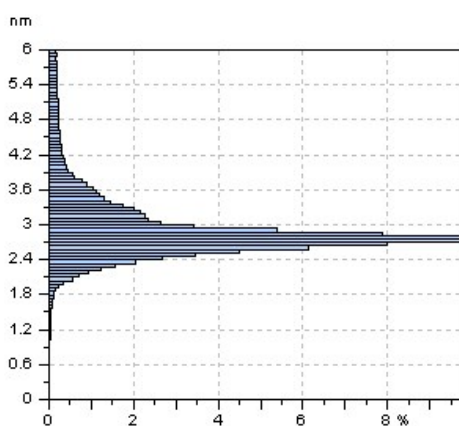


Figure S30: Statistical height distribution of **6**.

UV-visible spectrum of DHR **6**

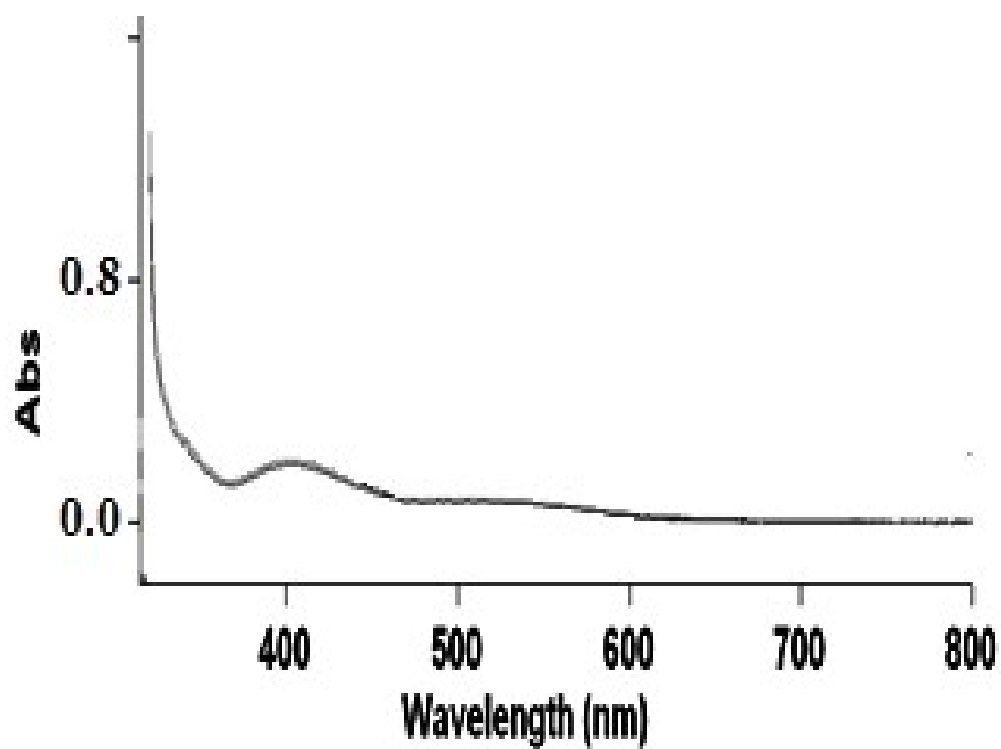


Figure S31: An absorption shoulder is observed at $\lambda_{\text{max}_1} = 408$ nm, and another absorption shoulder appears at $\lambda_{\text{max}_2} = 524$ nm, both corresponding to the product **6**.

IR (KBr) of DHR 6

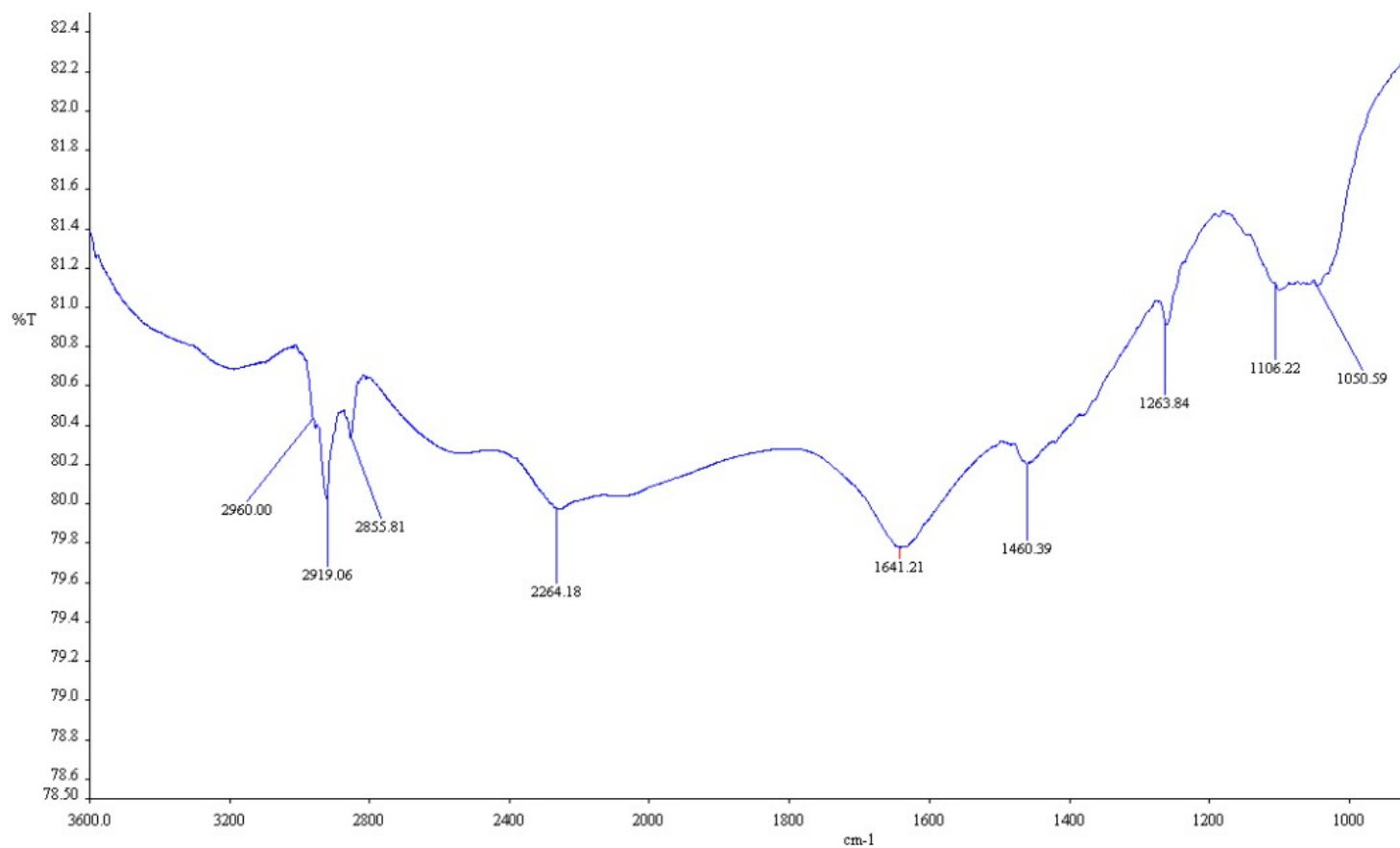


Figure S32: IR (KBr) of 6: 3150, 2960, 2919, 2855, 2264, 1641, 1460, 1106, 1050 (cm⁻¹).

Dendrimer empty DHR 1 (Cl)

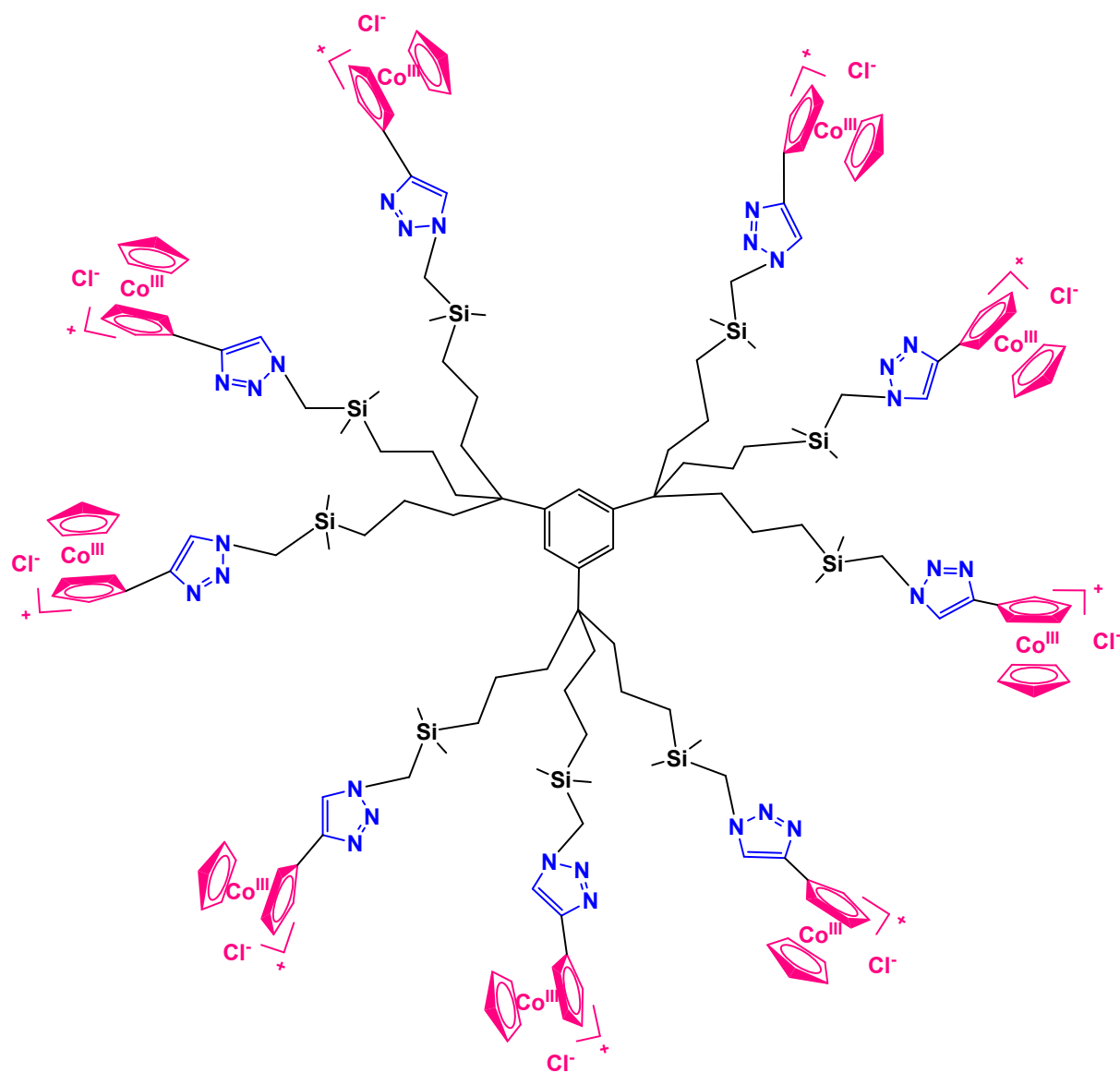


Figure S33: Structure of empty DHR 1(Cl⁻)

Experimental procedure for DHR 1(Cl)

The filled DHR 4 (10 mg, 0.003 mmol, 1 equiv.) was solubilized in 10 mL of THF. Then a 10 mL aqueous solution of HCl (0.03 mmol, 11 equiv.) was added dropwise, and the color gradually changed from deep red to light yellow giving back the empty DHR 1(Cl) and molecular hydrogen. After stirring for 10 min. the mixture of solvents was evaporated. Solubilization in water, filtration and evaporation of the solvent gave DHR 1(Cl) as a yellow waxy product in quantitative yield (11 mg). The empty DHR 1(Cl) is now water-soluble. ^1H NMR (1D 1H), (D_2O , 400 MHz) : δ_{ppm} : 8.39 (9H, CH of trz), 6.28 (18H, CH of Cp sub.), 5.91 (18H, CH of Cp sub.), 5.61 (45H, CH of Cp), 4.10 (18H, SiCH₂-trz), 1.34 (18H, CH₂CH₂CH₂Si), 0.88 (18H, CH₂CH₂CH₂Si), 0.47 (18H, 18H, CH₂CH₂CH₂Si), -0.04 (54H, Si(CH₃)₂). UV-vis.: $\lambda_{\text{max}1}$ = 356 nm, $\lambda_{\text{max}2}$ = 412 nm (shoulder).

^1H NMR spectroscopy of DHR 1(Cl)

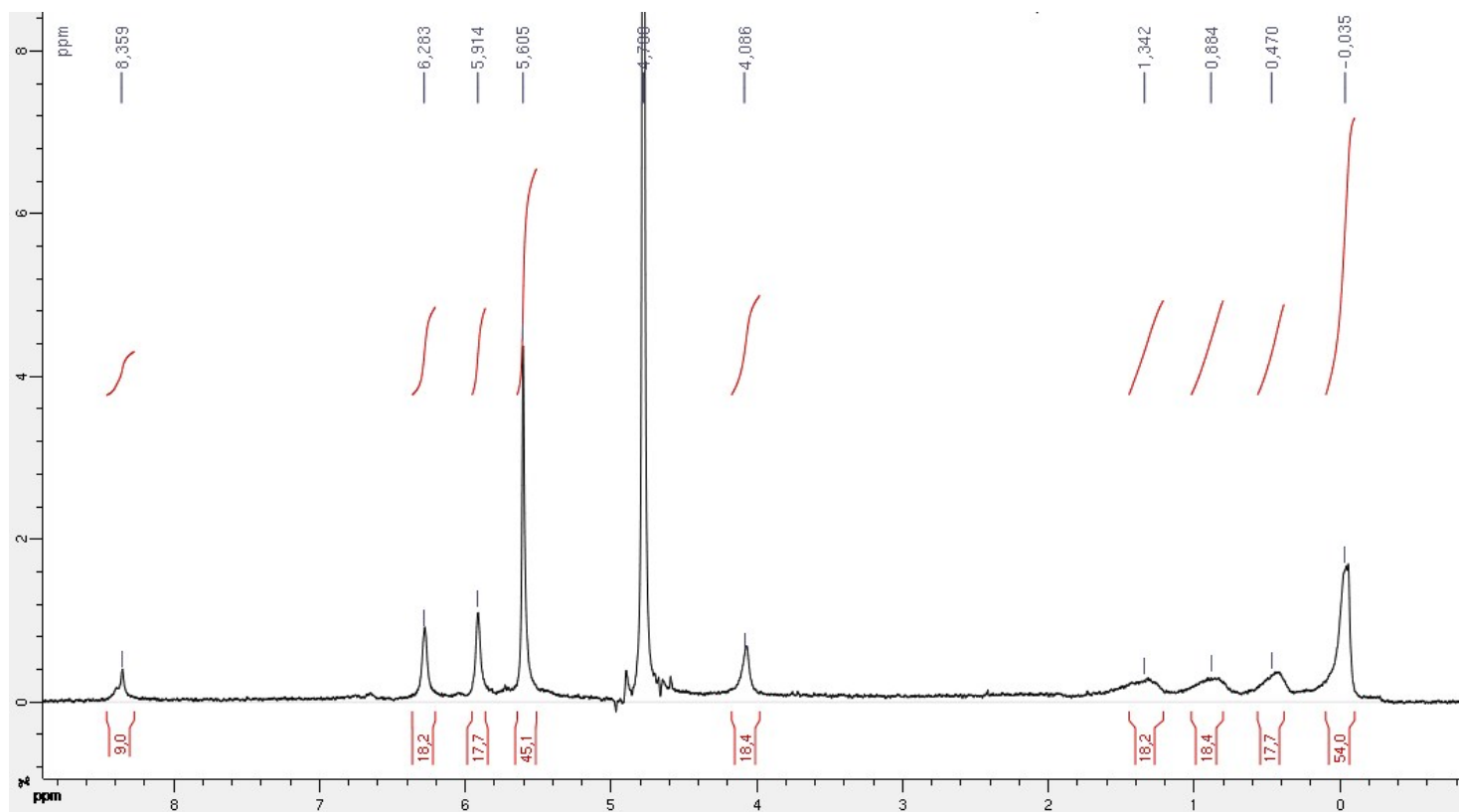


Figure S34: ^1H NMR spectrum of **1(Cl)** (1D 1H), (D_2O , 400 MHz) : δ_{ppm} : 8.39 (9H, CH of trz), 6.28 (18H, CH of Cp sub.), 5.91 (18H, CH of Cp sub.), 5.61 (45H, CH of Cp), 4.10 (18H, $\text{SiCH}_2\text{-trz}$), 1.34 (18H, $\text{CH}_2\text{CH}_2\text{CH}_2\text{Si}$), 0.88 (18H, $\text{CH}_2\text{CH}_2\text{CH}_2\text{Si}$), 0.47 (18H, 18H, $\text{CH}_2\text{CH}_2\text{CH}_2\text{Si}$), -0.04 (54H, $\text{Si}(\text{CH}_3)_2$).

UV-visible spectrum of DHR 1(Cl)

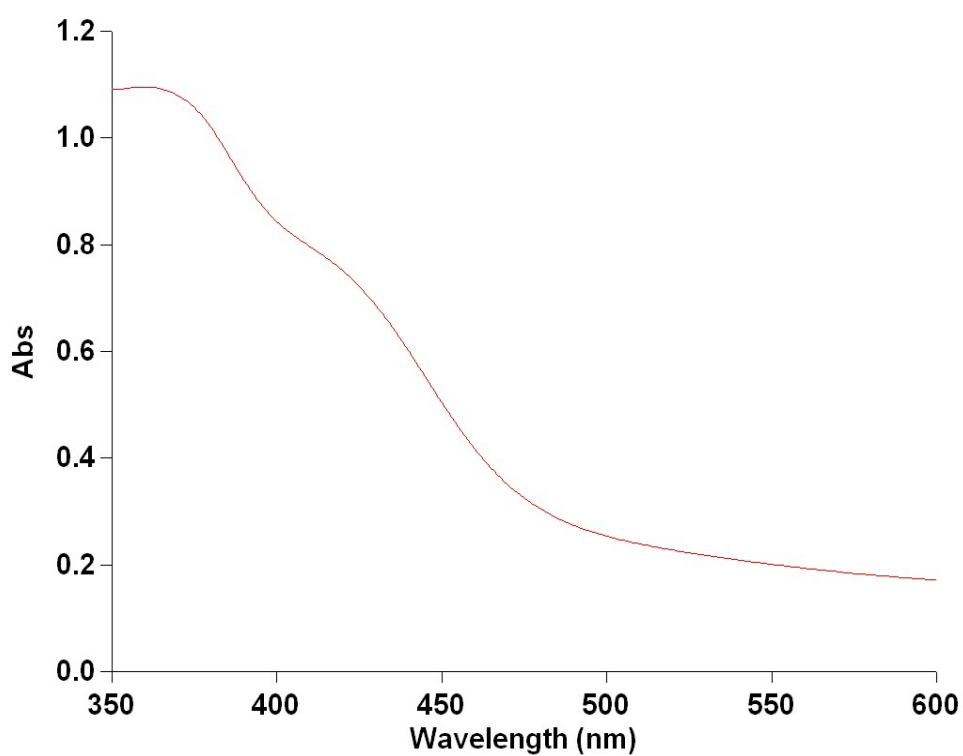


Figure S35: An absorption band is observed at $\lambda_{\text{max}_1} = 356$ nm and an absorption shoulder appears at $\lambda_{\text{max}_2} = 412$ nm corresponding to the product **1(Cl)**.

IR (KBr) of DHR 1(Cl)

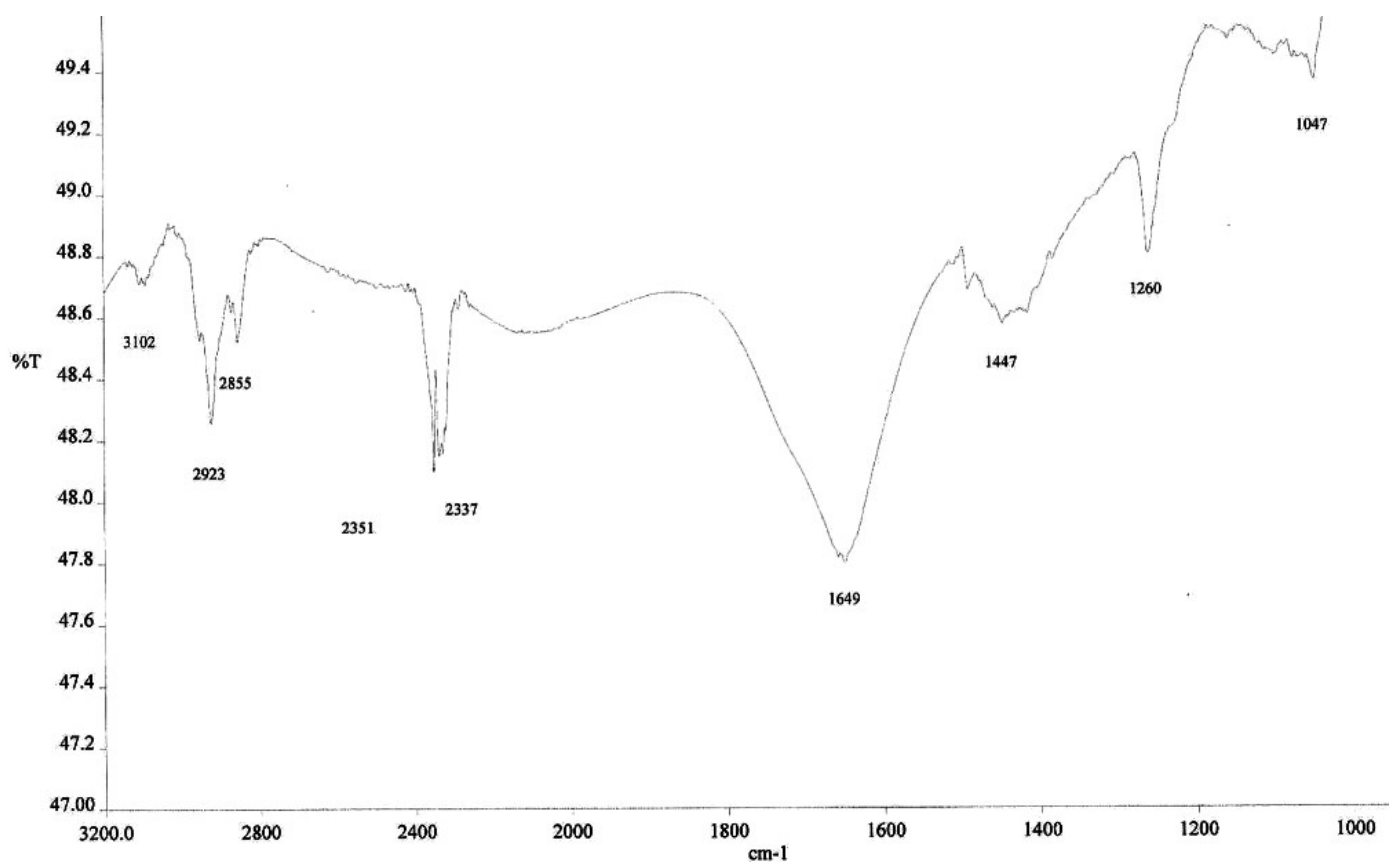


Figure S36: IR (KBr) of 1(Cl): 3102, 2923, 2855, 2337, 1649, 1447, 1260 (cm⁻¹).

Dendrimer empty 2(Cl)

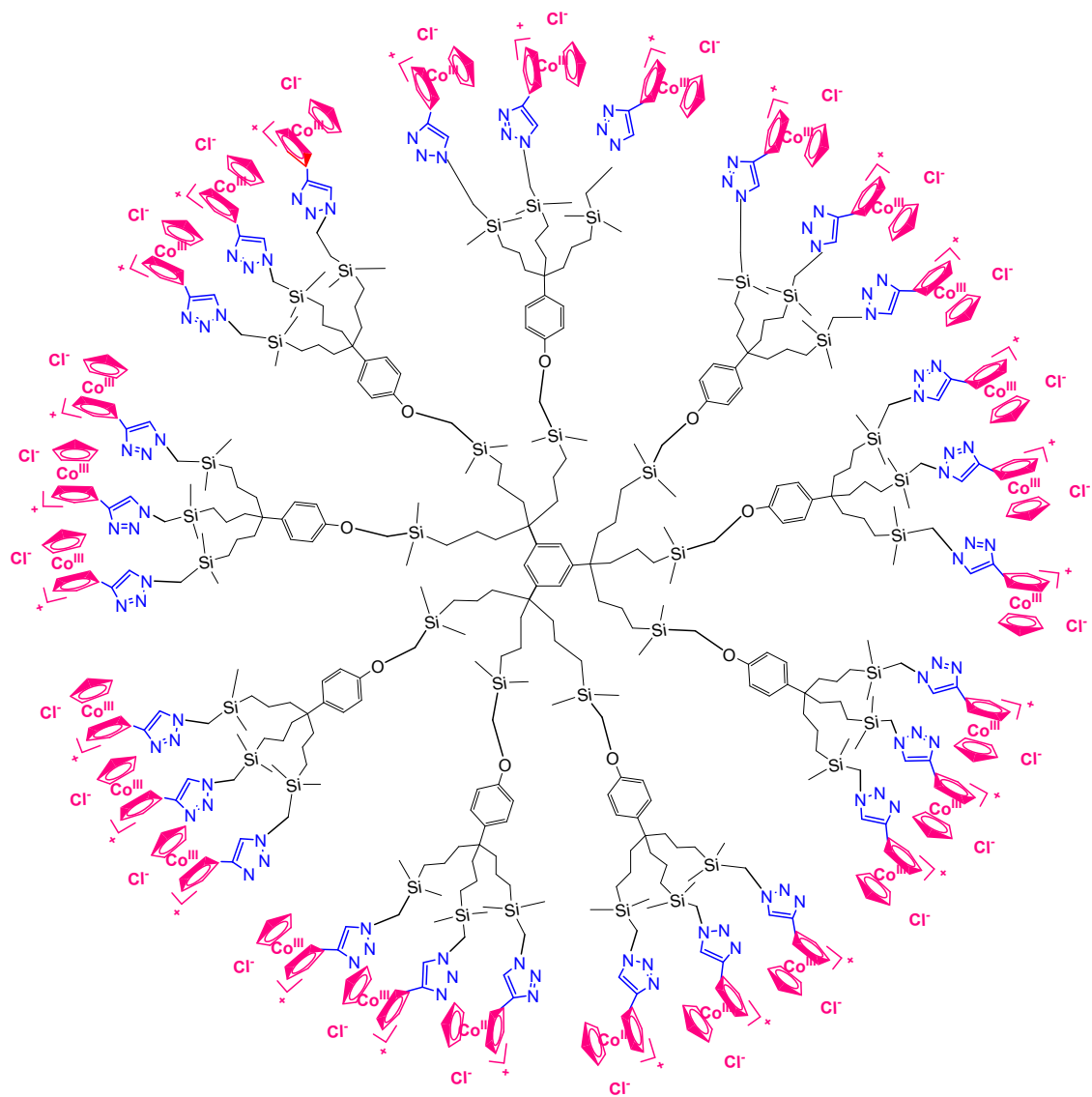


Figure S37: Structure of 2(Cl).

Experimental procedure for 2(Cl)

The filled DHR **5** (20 mg, 0.002 mmol, 1 equiv.) was solubilized in 10 mL of THF. Then a 10 mL aqueous solution of HCl (0.06 mmol, 33 equiv.) was added dropwise, and the color gradually changed from deep red to light yellow giving back the empty DHR **2(Cl)** and molecular hydrogen. After stirring for 10 min. the mixture of solvents was evaporated. Solubilization in water, filtration and evaporation of the solvent gave DHR **2(Cl)** as a yellow waxy product in quantitative yield (25 mg). The empty DHR **2(Cl)** is now water-soluble. ¹H NMR (1D 1H), (D₂O, 400 MHz): δ_{ppm}: 8.28 (27H, CH of trz), 7.00, 6.66 (39H, CH of arom.core), 6.09 (54H, CH of Cp sub.), 5.72 (54H, CH of Cp sub.), 5.39 (135H, CH of Cp), 3.90 (54H, SiCH₂-trz), 3.43 (18H, SiCH₂O), 1.44 (72H, CH₂CH₂CH₂Si), 0.94 (72H, CH₂CH₂CH₂Si), 0.39 (72H, 18H, CH₂CH₂CH₂Si), -0.14 (216H, Si(CH₃)₂). UV-vis.: λ_{max1} = 357 nm, λ_{max2} = 410 nm (shoulder).

UV-visible spectrum of DHR **2(Cl)**

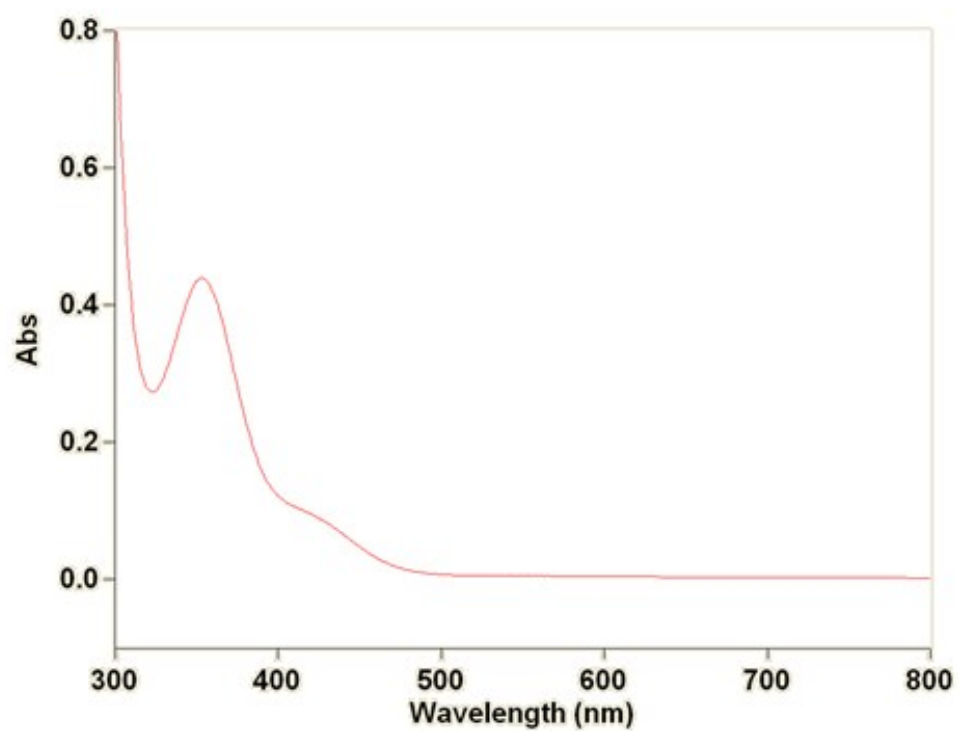


Figure S38: An absorption band is observed at $\lambda_{\max_1} = 357$ nm, and an absorption shoulder appears at $\lambda_{\max_2} = 410$ nm corresponding to the product **2(Cl)**.

^1H NMR of DHR 2(Cl)

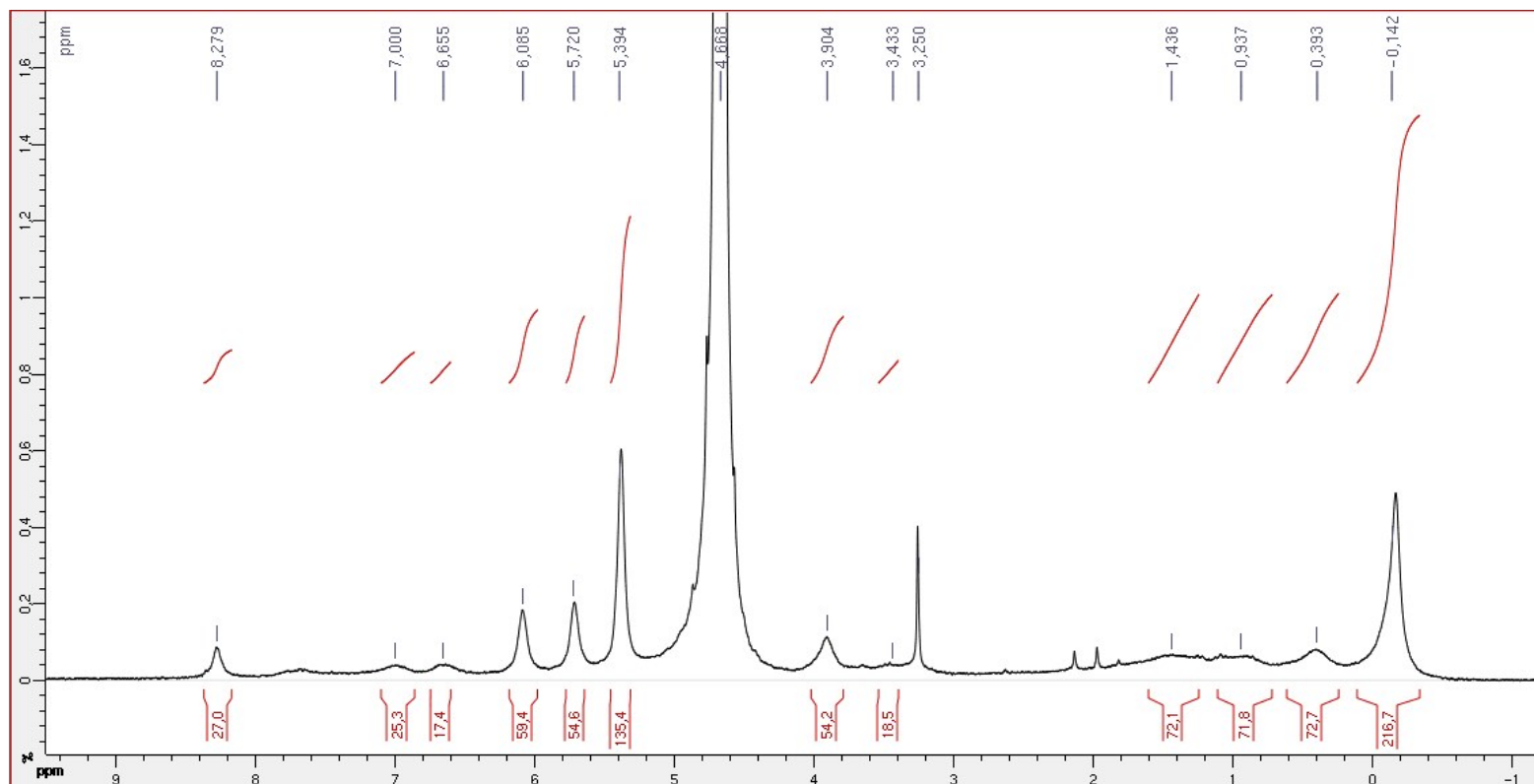


Figure S39: ^1H NMR spectrum of **2(Cl)** (1D 1H), (D_2O , 400 MHz): 8.28 (27H, CH of trz), 7.00, 6.66 (39H, CH of arom.core), 6.09 (54H, CH of Cp sub.), 5.72 (54H, CH of Cp sub.), 5.39 (135H, CH of Cp), 3.90 (54H, $\text{SiCH}_2\text{-trz}$), 3.43 (18H, SiCH_2O), 1.44 (72H, $\text{CH}_2\text{CH}_2\text{CH}_2\text{Si}$), 0.94 (72H, $\text{CH}_2\text{CH}_2\text{CH}_2\text{Si}$), 0.39 (72H, 18H, $\text{CH}_2\text{CH}_2\text{CH}_2\text{Si}$), -0.14 (216H, $\text{Si}(\text{CH}_3)_2$).

Dendrimer empty DHR 3(Cl)

Experimental procedure for DHR 3 (Cl)

The filled DHR **6** (15 mg, 0.4×10^{-3} mmol, 1 equiv.) was solubilized in 5 mL of THF. Then a 10 mL aqueous solution of HCl (0.04 mmol, 97 equiv.) was added dropwise, and the color gradually changed from deep red to light yellow giving back the empty DHR **3(Cl)** and molecular hydrogen. After stirring for 10 min. the mixture of solvents was evaporated. Solubilization in water, filtration and evaporation of the solvent gave DHR **3(Cl)** as a yellow waxy product in quantitative yield (15 mg). The empty DHR **3(Cl)** is now water-soluble. ^1H NMR (1D 1H), (D_2O , 400 MHz): δ_{ppm} : 8.35 (81H, *CH* of trz), 7.09, 6.76 (147H, *CH* arom.), 6.18 (162H, *CH* of Cp sub.), 5.80 (162H, *CH* of Cp sub.), 5.49 (405H, *CH* of Cp), 4.02 (162H, $\text{SiCH}_2\text{-trz}$), 3.51 (72H, SiCH_2O), 1.51 (234H, $\text{CH}_2\text{CH}_2\text{CH}_2\text{Si}$), 1.00 (234H, $\text{CH}_2\text{CH}_2\text{CH}_2\text{Si}$), 0.51 (234H, 18H, $\text{CH}_2\text{CH}_2\text{CH}_2\text{Si}$), -0.13 (702H, $\text{Si}(\text{CH}_3)_2$). UV-vis.: $\lambda_{\text{max}1} = 355$ nm, $\lambda_{\text{max}2} = 412$ nm (shoulder).

^1H NMR of DHR 3(Cl)

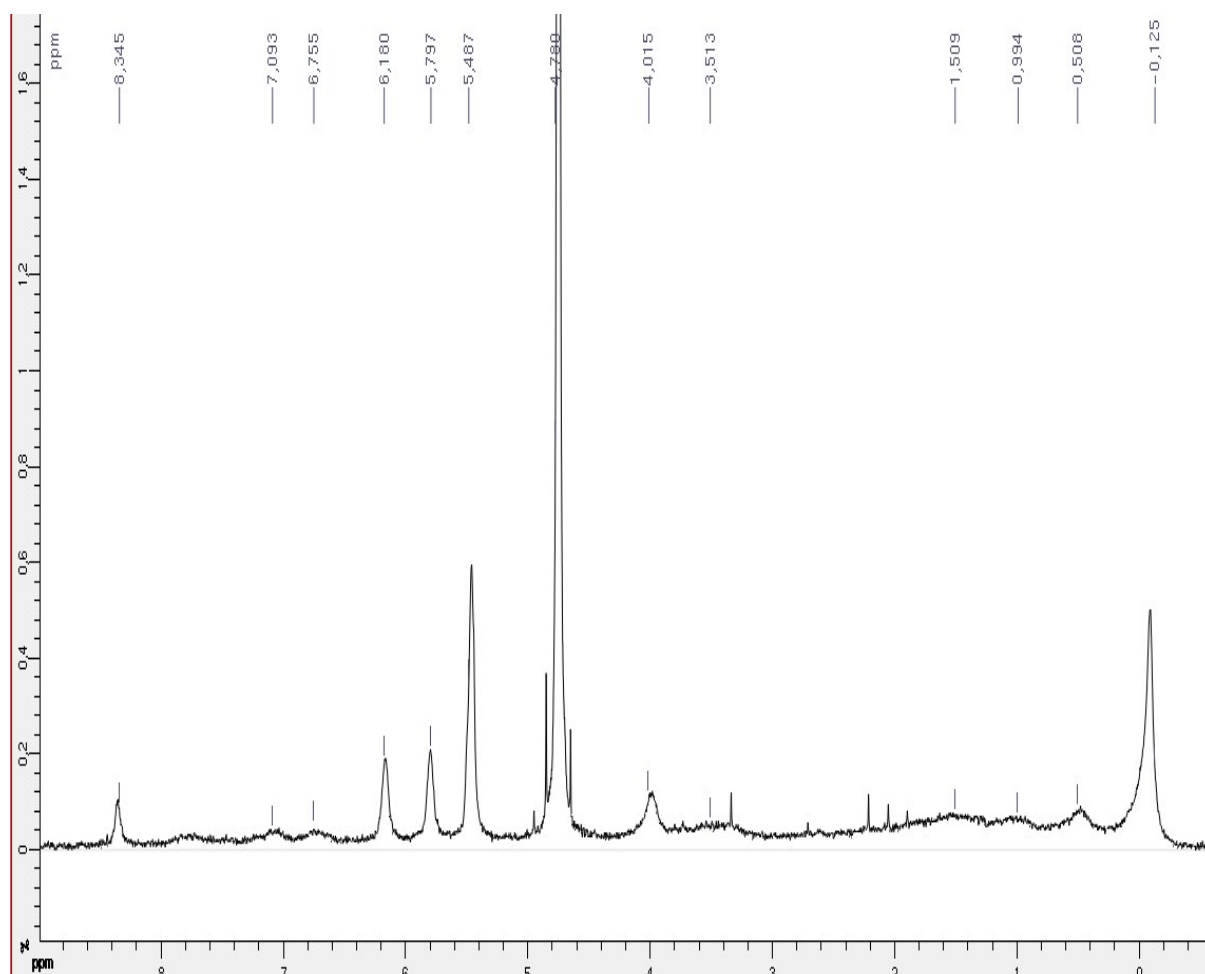


Figure S41: ^1H NMR spectrum of **3** (Cl) (1D 1H), (D_2O , 400 MHz): δ_{ppm} : 8.35 (81H, CH of trz), 7.09, 6.76 (147H, CH arom.), 6.18 (162H, CH of Cp sub.), 5.80 (162H, CH of Cp sub.), 5.49 (405H, CH of Cp), 4.02 (162H, $\text{SiCH}_2\text{-trz}$), 3.51 (72H, SiCH_2O), 1.51 (234H, $\text{CH}_2\text{CH}_2\text{CH}_2\text{Si}$), 1.00 (234H, $\text{CH}_2\text{CH}_2\text{CH}_2\text{Si}$), 0.51 (234H, 18H, $\text{CH}_2\text{CH}_2\text{CH}_2\text{Si}$), -0.13 (702H, $\text{Si}(\text{CH}_3)_2$).

UV-visible spectrum of DHR 3(Cl)

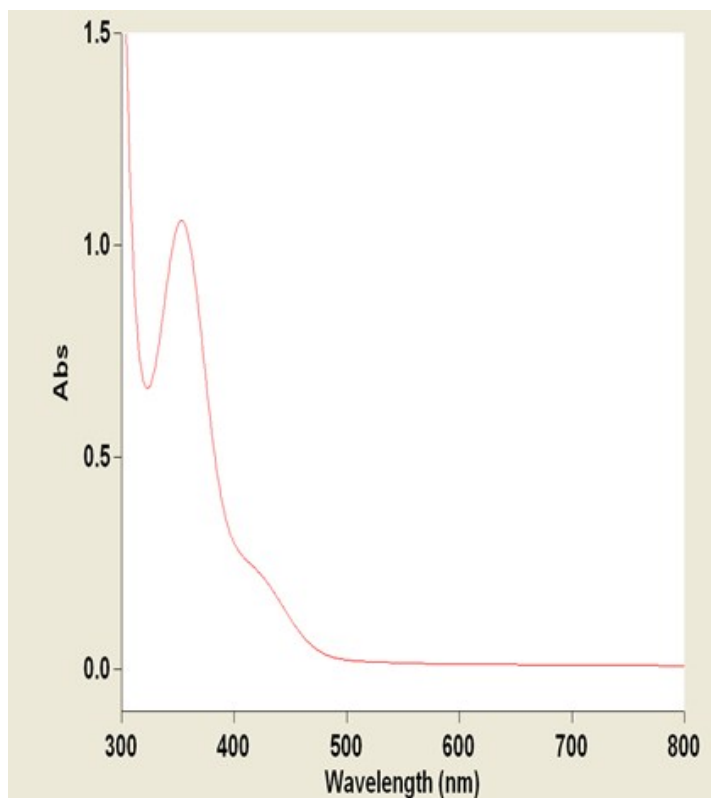
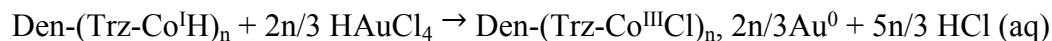


Figure S42: An absorption band observed at $\lambda_{\max_1} = 355$ nm and an absorption shoulder at $\lambda_{\max_2} = 412$ nm corresponding to product **3 (Cl)**.

AuNPs-7 and AuNPs-8

General information:

1) The **AuNPs-7** and **AuNPs-8** were synthesized according to the following equation:



2) After the reaction the pH was found to be acidic: **pH = 5-6**

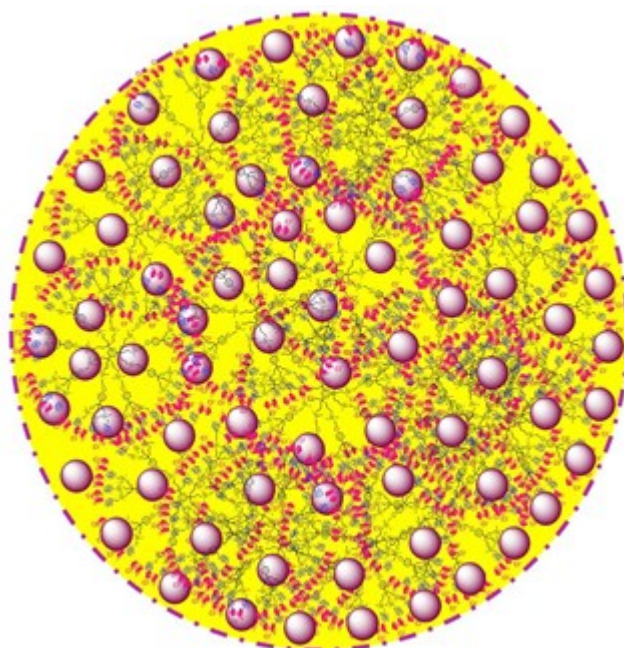


Figure S43: Schematic representation of capsules containing **AuNPs-7** or **AuNPs-8**.

3) Upon synthesis, the color immediately became **pink-red**:



Figure S45: Photograph of **AuNPs-8**.

4) A test has been performed using a flux of hydrogen gas into a solution of HAuCl_4 , and reduction of Au(III) to Au(0) started to occur after 15 minutes, proving that the hydride transfer from filled DHRs **4** and **5** to Au(III) is responsible for the Au(III) reduction to AuNPs. The consumption of both starting materials stoichiometrically as well as the remaining acidic pH confirm the above statement.

Experimental procedure of AuNPs-7

The filled DHR **4** (8 mg, 0.002 mmol, 1 equiv.) was dissolved in 1.5 mL THF and was added dropwise at 0°C into a solution of H₂AuCl₄ (4.7 mg, 0.012 mmol, 18 equiv.) in 35 mL of H₂O/ THF 3:1, under vigorous stirring. The color instantaneously changed from yellow to pink red, and stirring was continued for another 10 min. The mixture was concentrated *in vacuo* to 25 mL. UV-vis.: $\lambda_{\max} = 351$ nm, SPR: $\lambda_{\max} = 534$ nm. TEM: $d_{\text{AuNPs}} = 4.5 \pm 0.5$ nm, $d_{\text{Capsules}} = 45 \pm 7$ nm.

Experimental procedure of AuNPs-8

The filled DHR **5** (10 mg, 0.8×10^{-3} mmol, 1 equiv.) was dissolved in 1 mL THF and was added dropwise at 0°C in a solution of H₂AuCl₄ (5.7 mg, 0.014 mmol, 18 equiv.) in 40 mL of H₂O/ THF 3:1, under vigorous stirring. The color instantaneously changed from yellow to pink red, and stirring was continued for another 10 min. The mixture was concentrated *in vacuo* to 30 mL. UV-vis.: $\lambda_{\max} = 348$ nm, SPR: $\lambda_{\max} = 527$ nm. TEM: $d_{\text{AuNPs}} = 3 \pm 0.5$ nm, $d_{\text{Capsules}} = 85 \pm 20$ nm.

UV-vis. of AuNPs-7

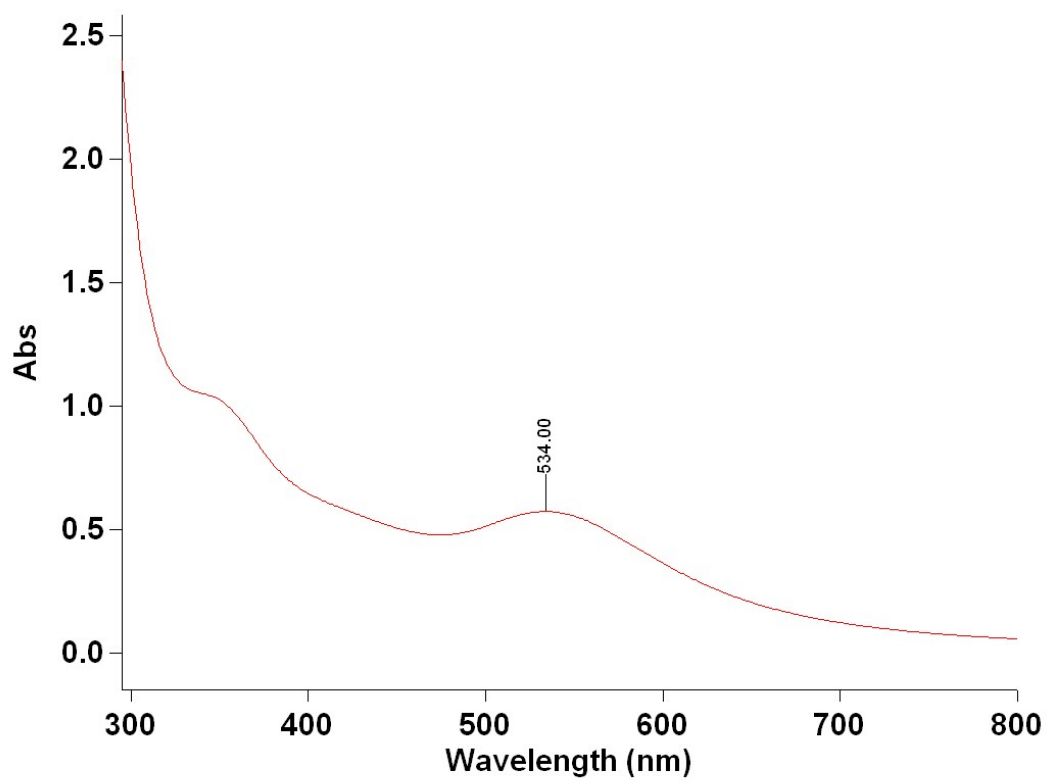


Figure S46: UV-vis. spectrum of AuNPs-7.

$\lambda_{\max} = 347 \text{ nm}$, SPR: $\lambda_{\max} = 534 \text{ nm}$

TEM of AuNPs-7

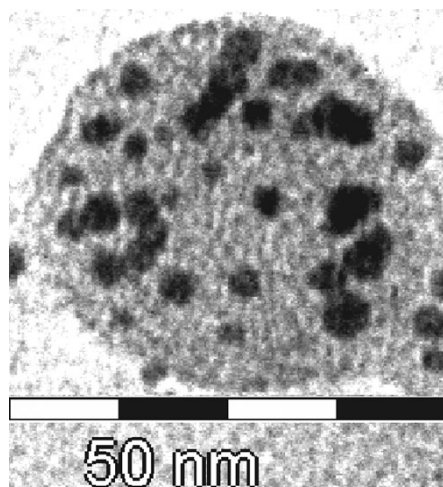


Figure S47: TEM image of **AuNPs-7**. The diameter of the AuNPs is: $d_{\text{AuNPs}} = 4.5 \pm 0.5$ nm, and that of the capsules is: $d_{\text{Capsules}} = 45 \pm 7$ nm.

Size distribution of AuNPs-7

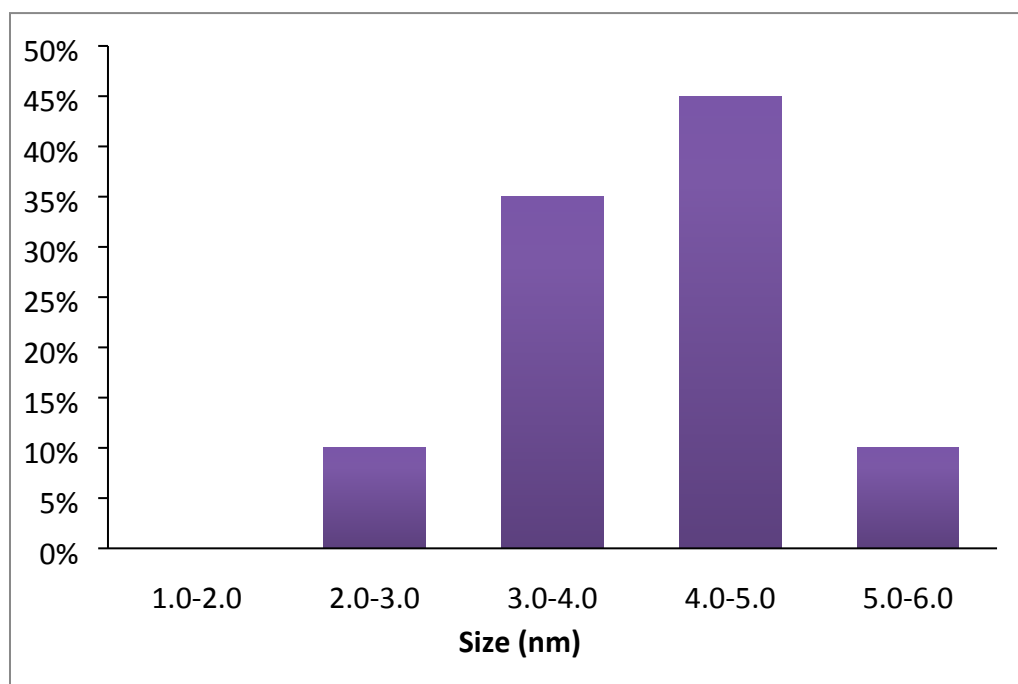
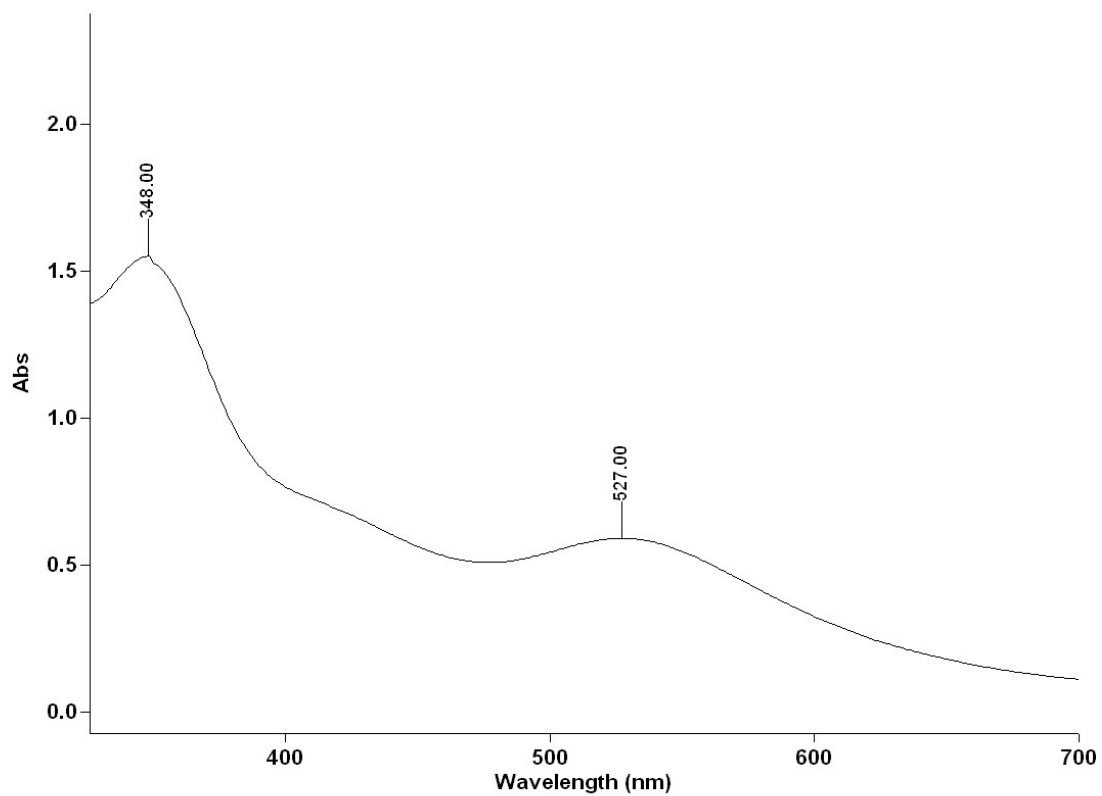


Figure S48.

UV-vis. of AuNPs-8



S49: UV-vis. spectrum of **AuNPs-8**.

$\lambda_{\max} = 348 \text{ nm}$, SPR: $\lambda_{\max} = 527 \text{ nm}$

Size distribution of AuNPs-8

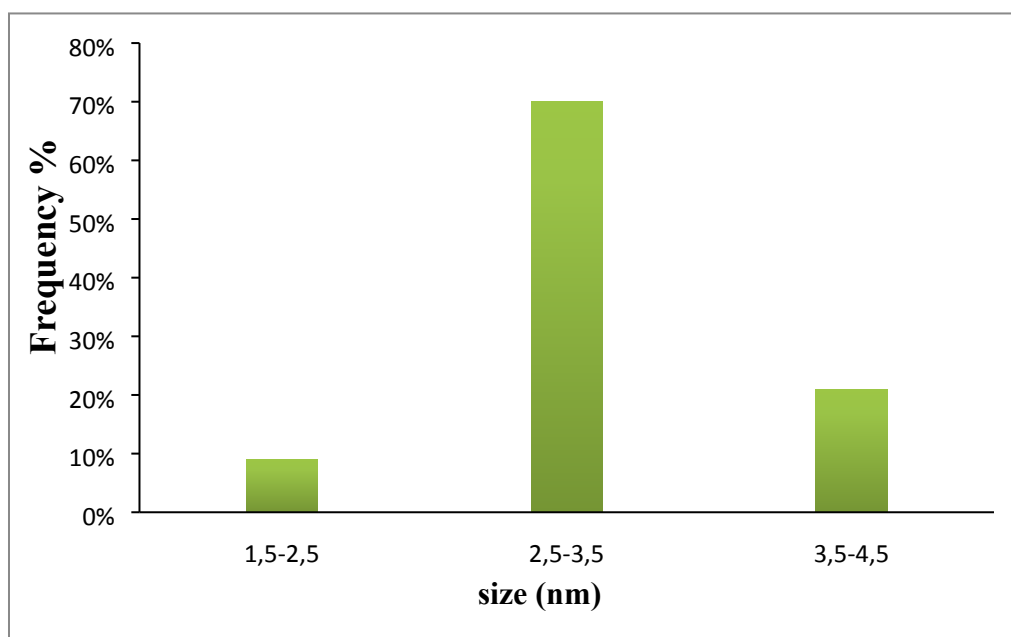


Figure S50.

AFM studies of AuNPs-8

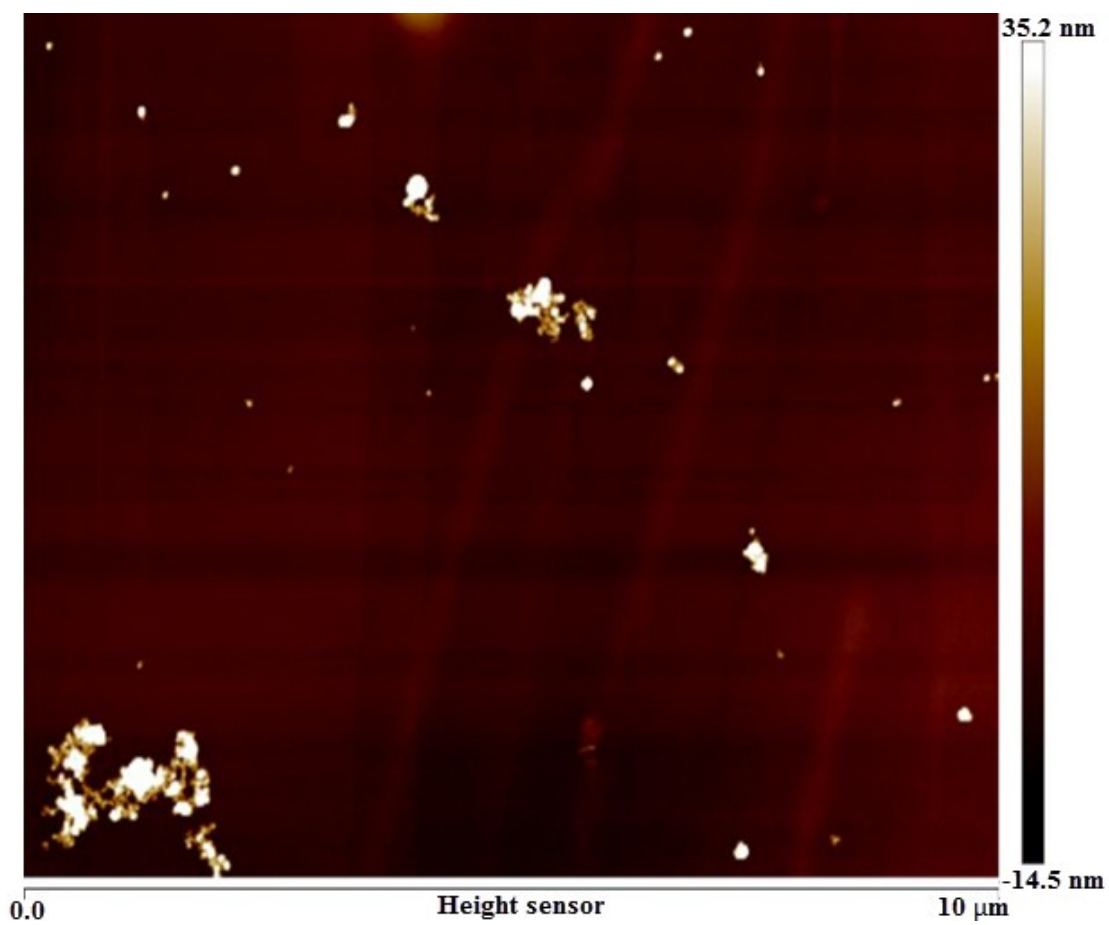


Figure S51: AFM image (height sensor) of AuNPs-8 at a larger scale (10 μm) where packages of capsules are also observed.

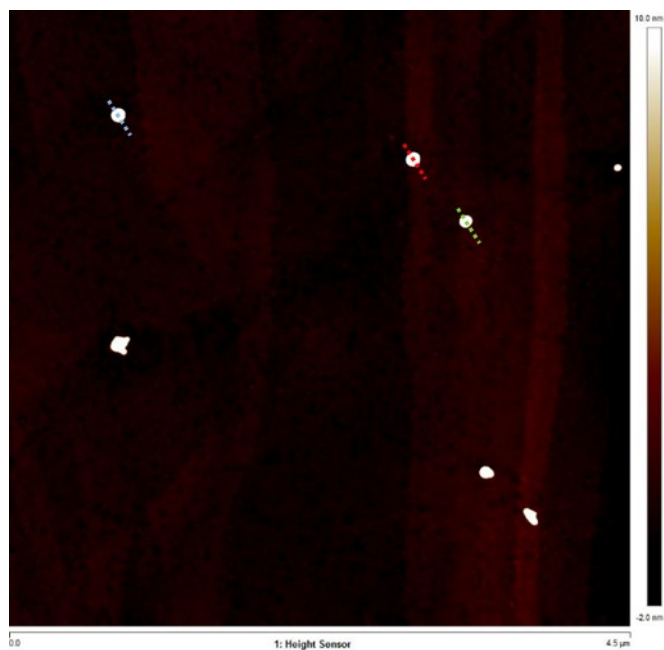


Figure S52: Calculation of distinct capsules' diameter and height containing **AuNPs-8** by AFM topography image ($d_{\text{Capsules}} = 103 \pm 14$ nm, $h_{\text{Capsules}} = 33 \pm 3$ nm) which is in agreement with TEM measurements ($d_{\text{Capsules}} = 85 \pm 20$ nm).
AuNPs-9

General information:

1) The **AuNPs-9** were synthesized according to the following equation:

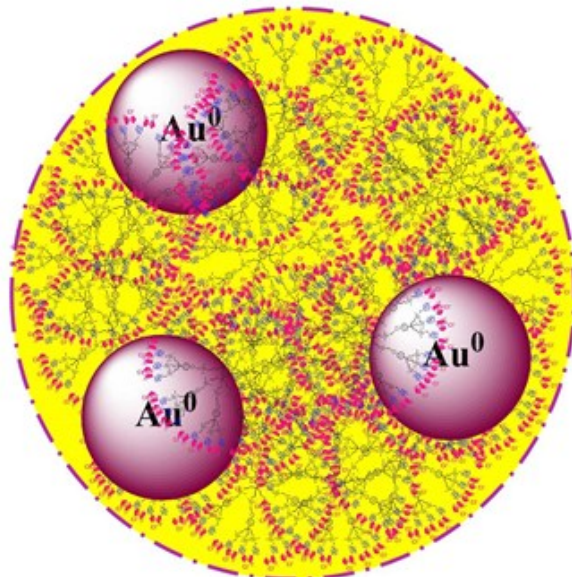
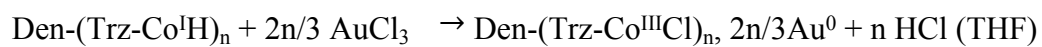


Figure S53: Schematic representation of capsules containing **AuNPs-9**.

2) The color changed immediately from yellow to **purple**:



Figure S54: Photo of **AuNPs-9**.

3) The fact that the reaction happens instantaneously confirms that the hydride transfer reduces Au(III) (in this case there is no acidic protons).

Experimental procedure for AuNPs-9

The filled DHR **5** (10 mg, 0.8×10^{-3} mmol, 1 equiv.) was dissolved in 1 mL THF and added dropwise at 0°C into a solution of AuCl₃ (4.4 mg, 0.014 mmol, 18 equiv.) in 35 mL of THF, under vigorous stirring. The color instantaneously changed from yellow to violet, and stirring was continued for another 10 min. The mixture was kept in a closed flask. UV-vis.: $\lambda_{\text{max}} = 350$ nm, SPR: $\lambda_{\text{max}} = 571$ nm. TEM: $d_{\text{AuNPs}} = 33 \pm 3$ nm, $d_{\text{Capsules}} = 220 \pm 40$ nm.

Size distribution of AuNPs-9

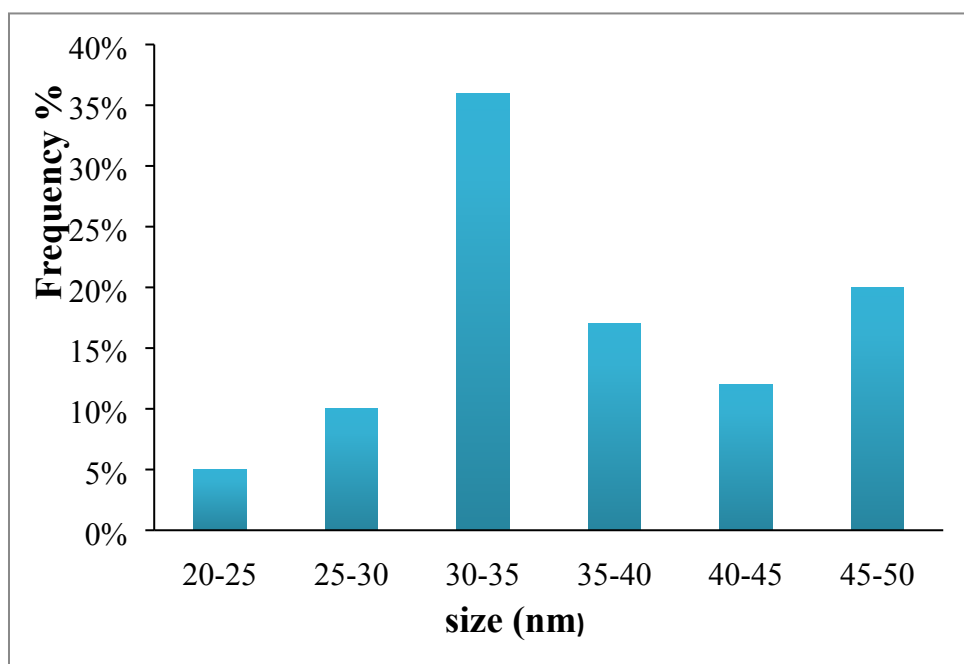


Figure S55

AuNPs-10

General information

For comparison a common reductant NaBH_4 was used to reduce HAuCl_4 to give **AuNPs-10** that were stabilized by the empty DHR 2 (Cl^-).

The reaction happened instantaneously and the color changed immediately from yellow to grey-purple.



Figure S56: Photo of AuNPs-10

From TEM analysis capsules were not observed, whereas comparative stability tests were performed.

The same concentration was used as in case of **AuNPs-8**, but under these conditions **AuNPs-10** flocculated. They could be reversibly re-dissolved, however.

The pH after the reaction becomes $\text{pH} = 7$.

Experimental procedure for AuNPs-10

The empty DHR **2(Cl)** (10 mg, 0.8×10^{-3} mmol, 1 equiv.) was dissolved in 4 mL H₂O and was added in a solution of HAuCl₄ (5.7 mg, 0.014 mmol, 18 equiv.) in 25 mL of H₂O, under vigorous stirring. Then a solution of NaBH₄ (1.7 mg, 0.04 mmol, 54 equiv.) in 1 mL H₂O was added dropwise under vigorous stirring. The color instantaneously changed from yellow to grey-purple and stirring was continued for another 10 min. UV-vis.: $\lambda_{\max} = 348$ nm, SPR: $\lambda_{\max} = 535$ nm. TEM: $d_{\text{AuNPs}} = 5 \pm 1$ nm.

TEM of AuNPs-10

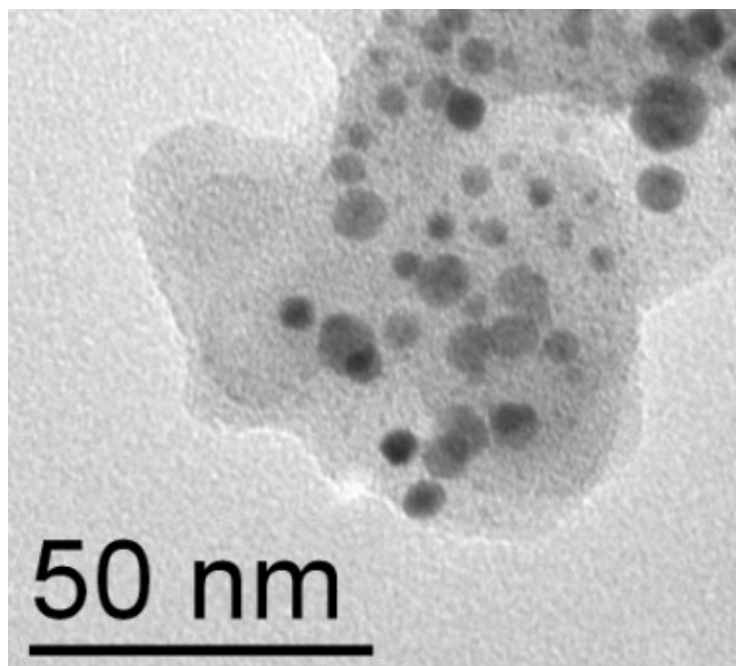


Figure S57: TEM image of AuNPs-10. The calculated diameter was found: $d = 5 \pm 1$ nm.

Size distribution of AuNPs-10

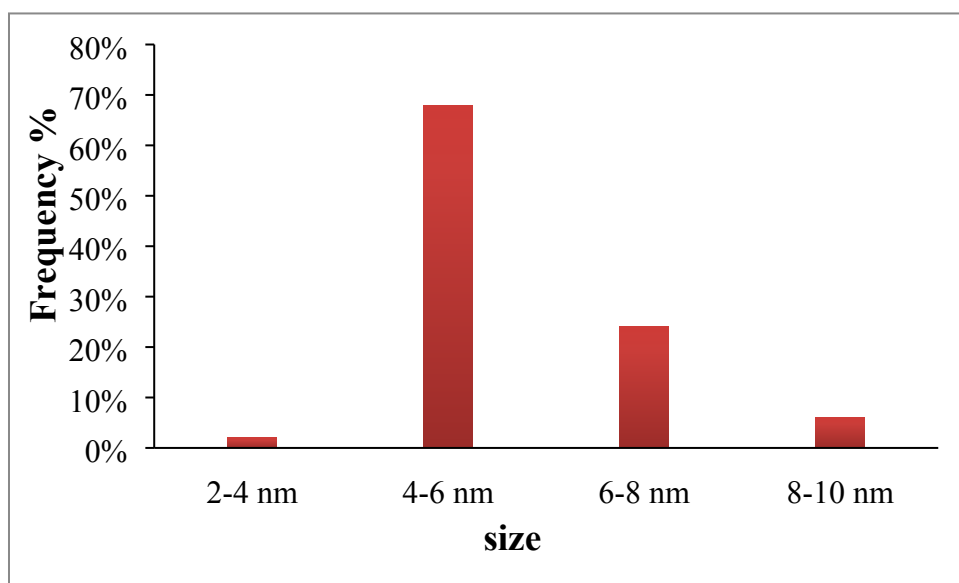


Figure S58

UV-vis. of AuNPs-10

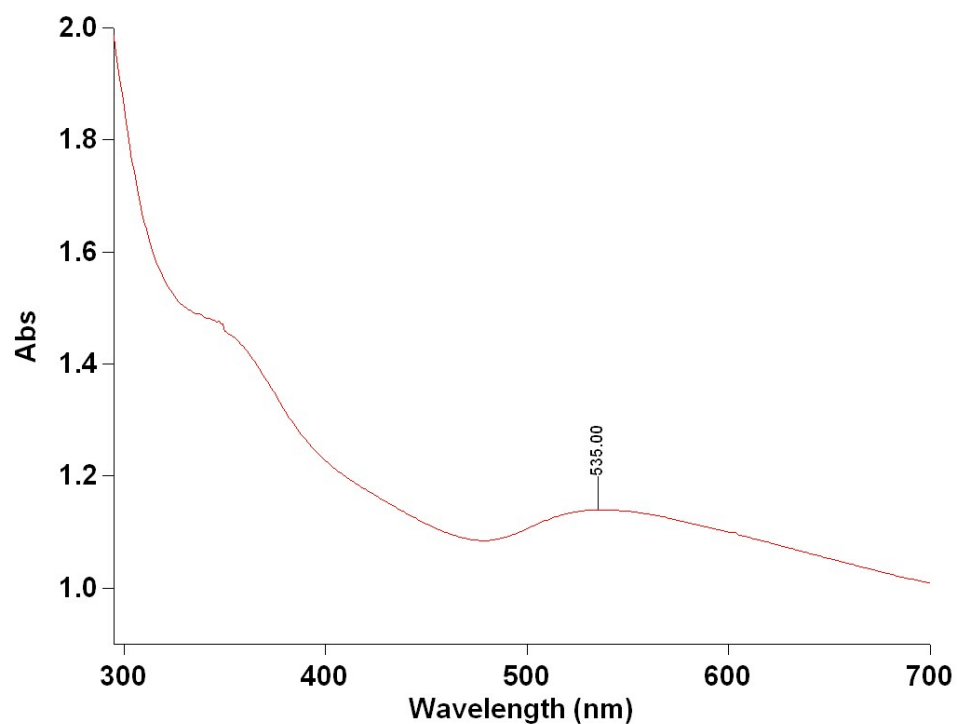


Figure S59: UV-vis. spectrum of AuNPs-10.

$\lambda_{\max} = 348 \text{ nm}$, SPR: $\lambda_{\max} = 535 \text{ nm}$.

Stability comparison of AuNPs-8 and AuNPs-10

1) Time

The **AuNPs-8** were stable for several months. Precipitation did not occur, and the UV-vis. spectrum after several months showed the same plasmon band as when they were freshly prepared.

UV-vis of AuNPs-8 after 6 months

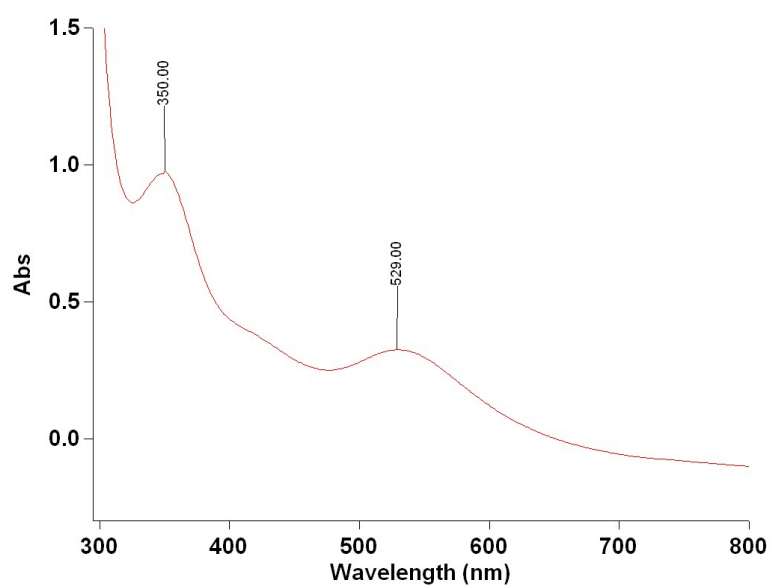


Figure S60: UV-vis. spectrum of AuNPs-8.

$\lambda_{\text{max}} = 350 \text{ nm}$, SPR: $\lambda_{\text{max}} = 529 \text{ nm}$.

On the other hand, **AuNPs-10** could not be re-dissolved after one month time, showing that their stability is weaker comparing to capsules containing **AuNPs-8**.

2) Temperature

Both **AuNPs-8** and **AuNPs-10** were heated at 100° C during one hour. After 30 min, **AuNPs-10** were irreversibly precipitated, whereas in the case of **AuNPs-8** nothing changed (color or solubility). The UV-vis. spectrum was recorded after heating **AuNPs-8** giving the same plasmon band as before heating.

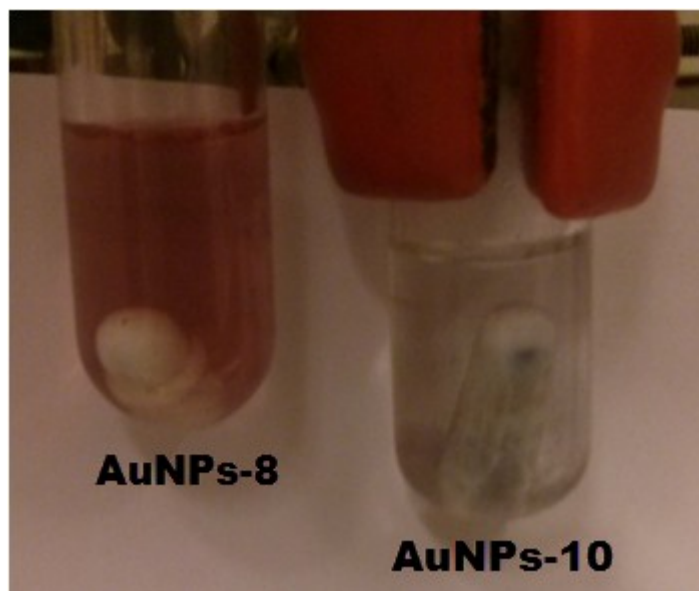


Figure S61: Photograph of **AuNPs-8** and **AuNPs-10** after heating at 100°C for 1h.

UV-vis. spectrum of AuNPs-8 after heating at 100°C during 1h

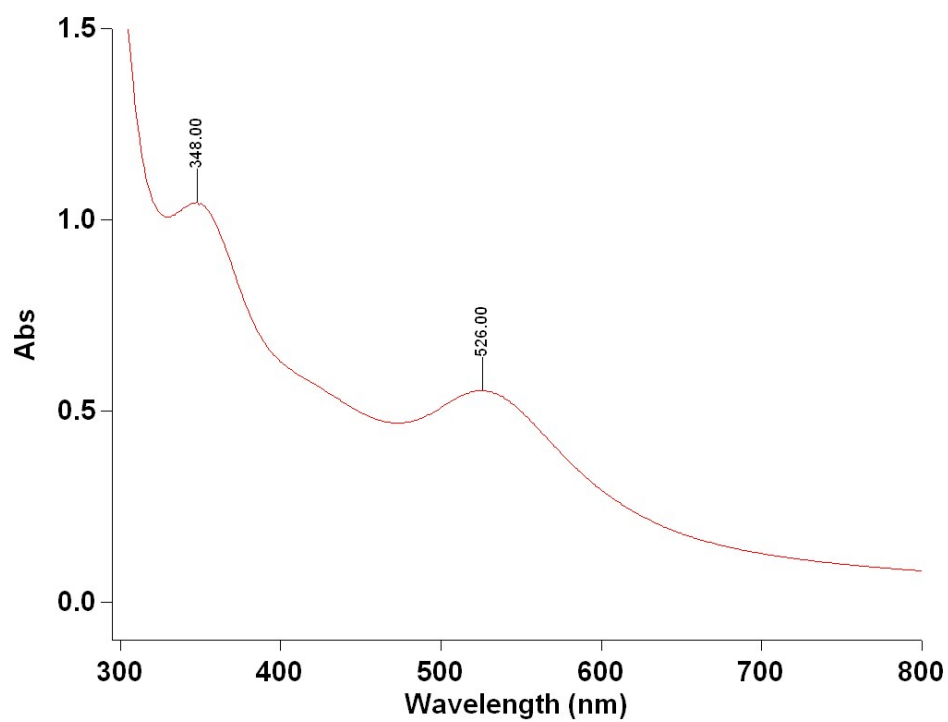


Figure S62: UV-vis. spectrum of AuNPs-8.

$\lambda_{\max} = 348 \text{ nm}$, SPR: $\lambda_{\max} = 526 \text{ nm}$.

AuNPs-11

A mixture of empty DHR **2** (PF_6^-) and AuCl_3 was reduced by NaBH_4 resulting in the simultaneous reduction of dendrimer **2** (PF_6^-) to the filled DHR **5** and Au(III) to Au(0) . The color changed from yellow to purple (instantaneous reduction of Au(III)) and subsequently to red when the empty DHR was reduced to filled DHR (**AuNPs-11**). After 5 min. the **AuNPs-11** flocculated which is taken into account by the absence of electrostatic stabilization and could be reversibly dissolved by stirring the reaction medium. These nanoparticles were kept under nitrogen.

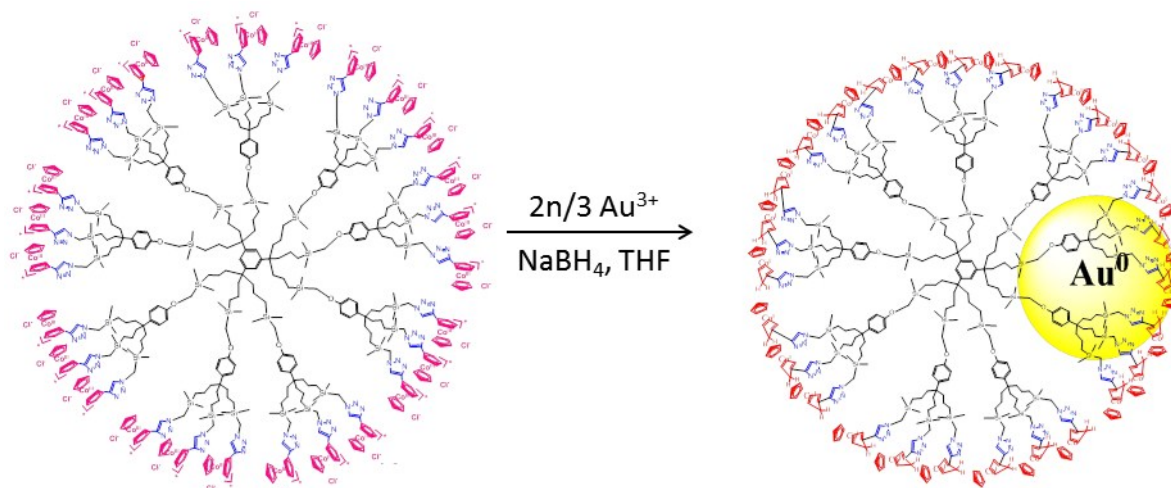


Figure S63: Synthesis of **AuNPs-11**.



Figure S64: Photo of **AuNPs-11**.

Experimental procedure for AuNPs-11

The empty DHR **2(PF₆)** (8 mg, 0.5×10^{-3} mmol, 1 equiv.) and AuCl₃ (2.8 mg, 0.009 mmol, 18 equiv.) were put in a flask, and 10 mL of distilled THF was added under nitrogen. Then NaBH₄ (2 mg, 0.05 mmol, 100 equiv.) was added, and the solution was left stirring vigorously for 10 min. The color instantaneously changed from yellow to purple and then gradually became red suggesting first the reduction of Au^{III} and then gradually the reduction of cobalticenium. The solution was quickly filtered. The flocculation of **AuNPs-11** was observed after 5 min. UV-vis.: $\lambda_{\text{max}} = 408$ nm (shoulder), SPR: $\lambda_{\text{max}} = 519$ nm. TEM: $d_{\text{AuNPs}} = 4 \pm 0.5$ nm.

UV-vis. of AuNPs-11

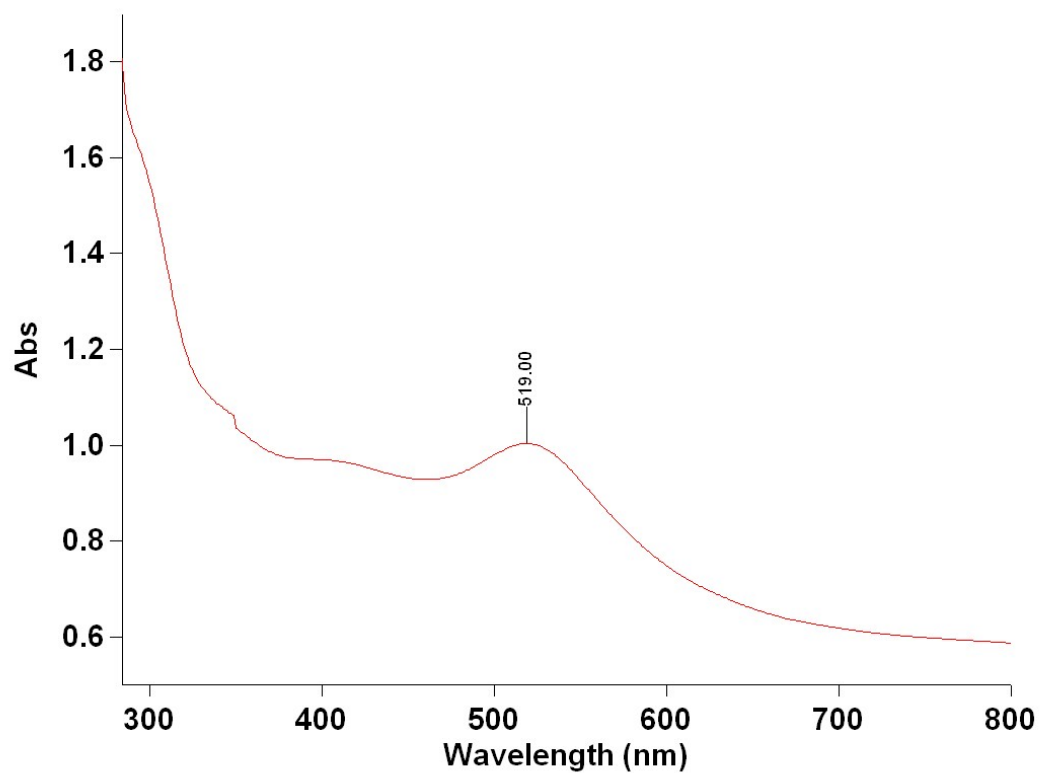


Figure S65: UV-vis. spectrum of AuNPs-11. Absorption shoulder: $\lambda_{\max} = 408$ nm. SPB: $\lambda_{\max} = 519$ nm.

TEM of AuNPs-11

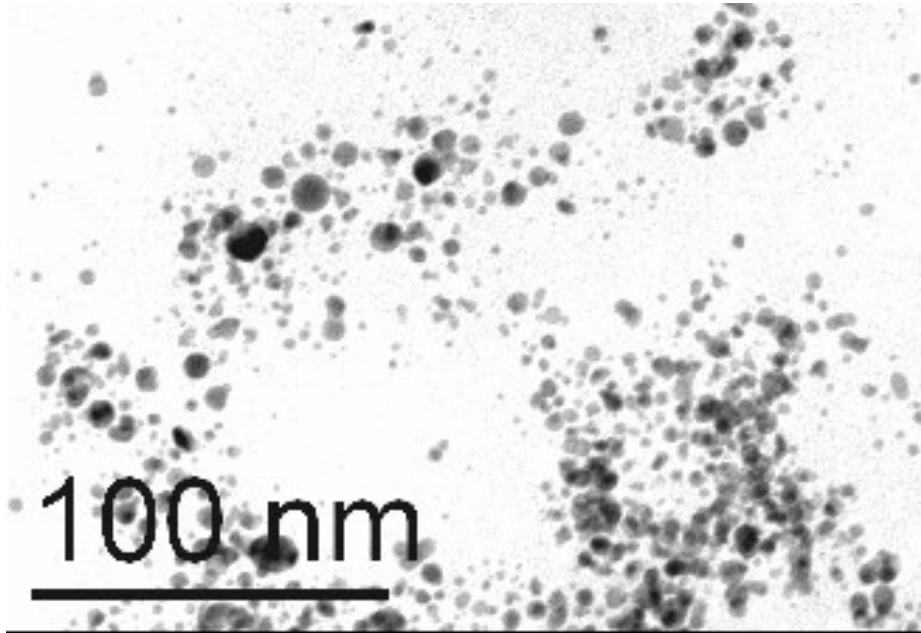


Figure S66: TEM image of flocculated AuNPs-11.

Size distribution of AuNPs-11

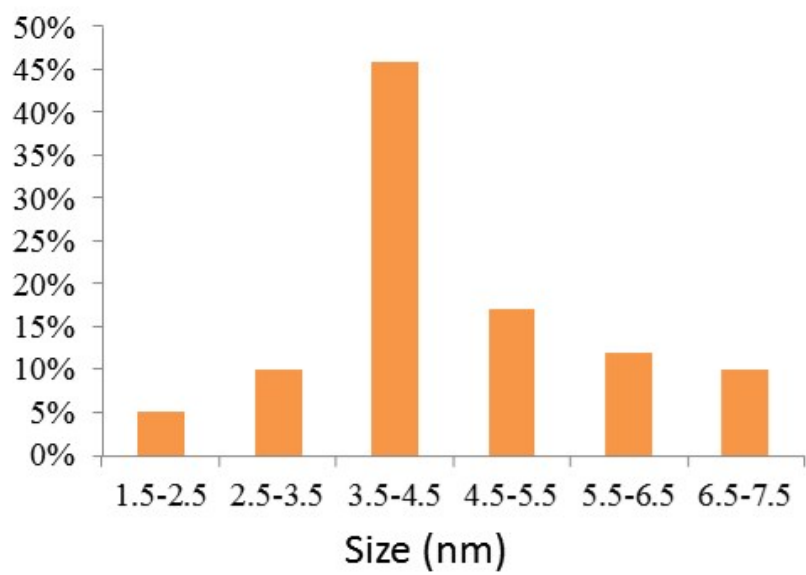


Figure S67

Oxidation of AuNPs-11 by HCl (AuNPs-12)

Experimental procedure for AuNPs-12

To the solution of **AuNPs-11** (S66) another 20mL of THF was added. Then a solution of HCl (0.02 mmol, 33 equiv.) in 10 mL of H₂O was added dropwise at 0°C under vigorous stirring and stirring continued for 10 min. AuNPs-12 were obtained in light orange/purple color. UV-vis.: $\lambda_{\max} = 356$ nm (shoulder), SPR: $\lambda_{\max} = 513$ nm. TEM: $d_{\text{AuNPs}} = 4 \pm 0.5$ nm.

TEM of AuNPs-12

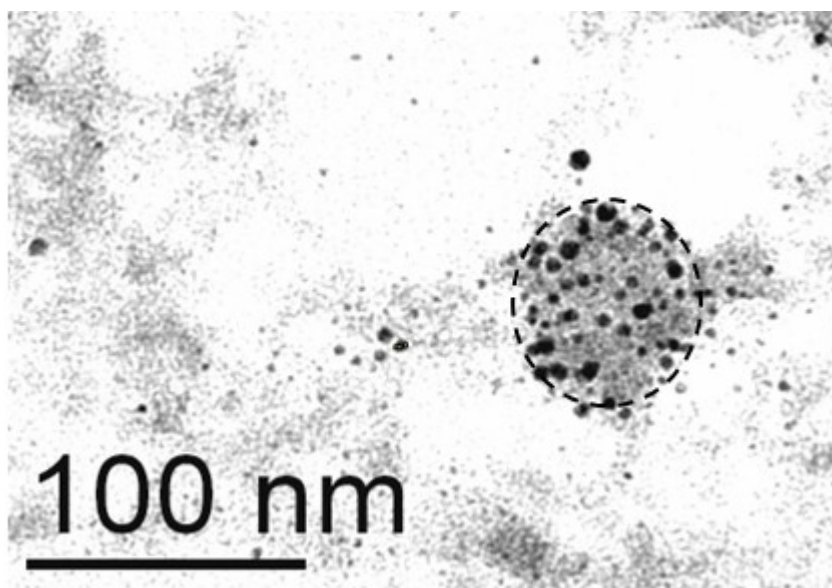


Figure S68: TEM image of AuNPs-12 stabilized by the cationic empty **DHR 2 (Cl)**. It is clearly seen that the re-arrangement of the AuNPs into capsules occurred when the filled **DHR 5** changed back to empty **DHR 2 (Cl)**.

Size distribution of AuNPs-12

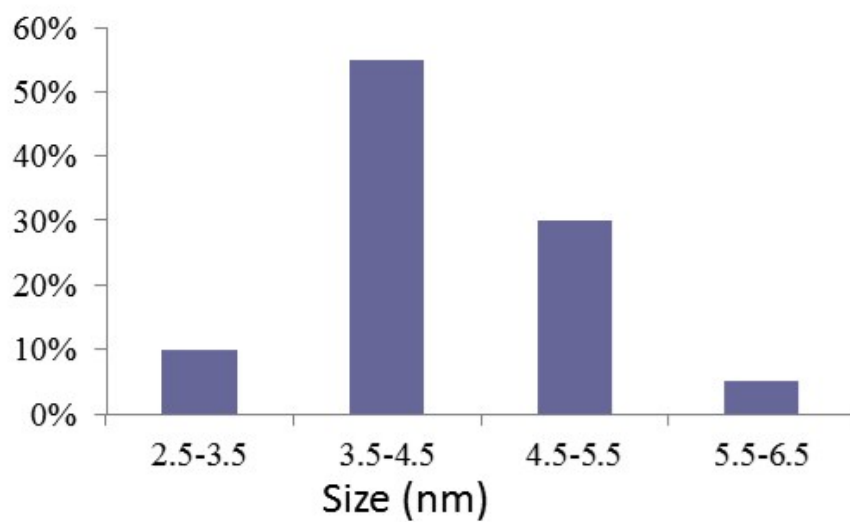


Figure S69

UV-vis. of AuNPs-12

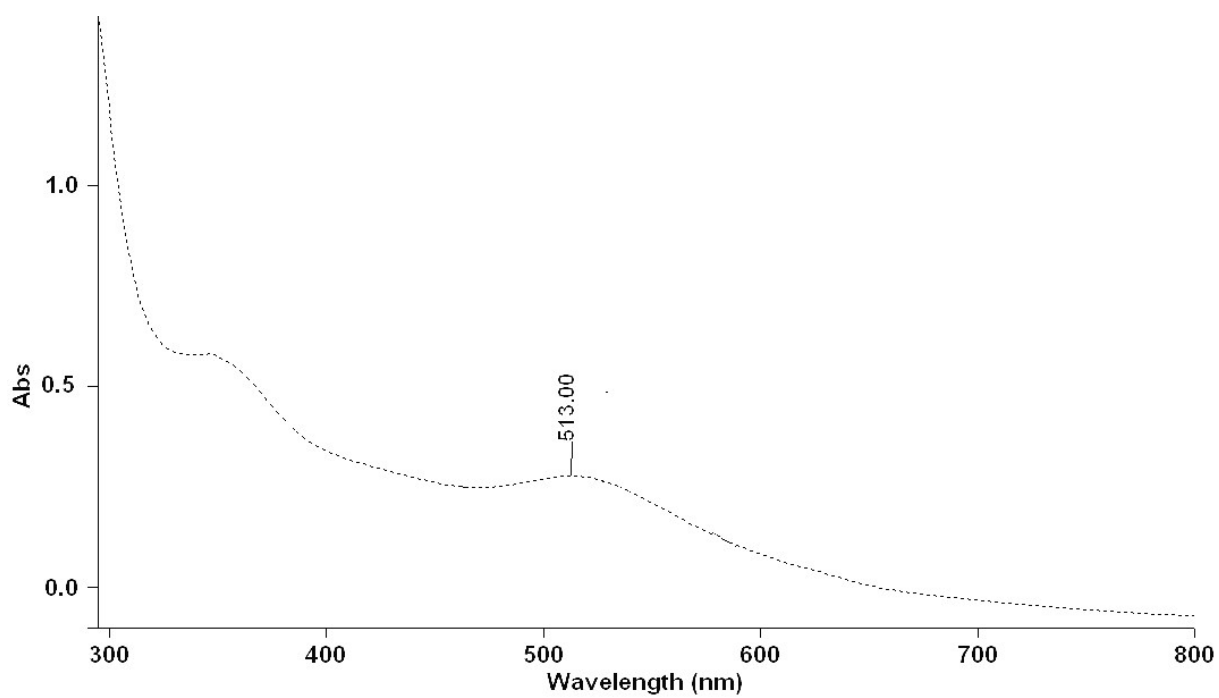


Figure S70: UV-vis. spectrum of AuNPs-12. Absorption: $\lambda_{\text{max}} = 357$ nm. SPB: $\lambda_{\text{max}} = 513$ nm.

References

- (1) A. Rapakousiou, C. Mouche, M. Duttine, J. Ruiz, D. Astruc, *Eur. J. Inorg. Chem.* **2012**, *31*, 5071-5077.
- (2) A. Rapakousiou, Y. Wang, C. Belin, N. Pinaud, J. Ruiz, D. Astruc, *Inorg. Chem.* **2013**, *52*, 6685-6693.
- (3) (a) C. Ornelas, J. Ruiz, C. Belin, D. Astruc, *J. Am. Chem. Soc.* **2009**, *131*, 590-601. (b) E. Boisselier, A. K. Diallo, L. Salmon, C. Ornelas, J. Ruiz, D. Astruc, *J. Am. Chem. Soc.* **2010**, *132*, 2729-2742. (c) R. Djeda, A. Rapakousiou, L. Liang, N. Guidolin, J. Ruiz, D. Astruc, *Angew. Chem., Int. Ed.* **2010**, *49*, 8152-8156.
- (4) O. A. Tarasova, I. V. Tatarinova, T. I. Vakul'skaya, S. S. Khutsishvili, V. I. Smirnov, L. V. Klyba, G. F. Prozorova, A. I. Mikhaleva, B. A. Trofimov, *J. Organomet. Chem.* **2013**, *1-7*, 745-746.
- (5) R. Ciganda, A. Garralda, L. Ibarlucea, E. Pinilla, R. Torres, *Dalton Trans.* **2010**, *39*, 7226-7229.